Mitochondrial haplotype mutation alleviates respiratory defect of MELAS by restoring taurine modification in tRNA with 3243A > G mutation

上田, 沙央理

7480–7495 *Nucleic Acids Research, 2023, Vol. 51, No. 14* *Published online 13 July 2023*
https://doi.org/10.1093/nar/gkad591

Mitochondrial haplotype mutation alleviates respiratory defect of MELAS by restoring taurine modification in tRNA with 3243A > G mutation

Saori Ueda[1], Mikako Yagi[1,2], Ena Tomoda[3], Shinya Matsumoto[1], Yasushi Ueyanagi[1], Yura Do[1], Daiki Setoyama[1], Yuichi Matsushima[1,4], Asuteka Nagao[3], Tsutomu Suzuki[3], Tomomi Ide[5], Yusuke Mori[6], Noriko Oyama[7], Dongchon Kang[1] and Takeshi Uchiumi[1,2,*]

[1]Department of Clinical Chemistry and Laboratory Medicine, Graduate School of Medical Sciences, Kyushu University, 3-1-1 Maidashi, Higashi-ku, Fukuoka 812-8582, Japan, [2]Department of Health Sciences, Graduate School of Medical Sciences, Kyushu University, 3-1-1 Maidashi, Higashi-ku, Fukuoka 812-8582, Japan, [3]Department of Chemistry and Biotechnology, Graduate School of Engineering, University of Tokyo, 7-3-1 Hongo, Bunkyo-ku, Tokyo 113-8656, Japan, [4]Department of Biological Sciences, Graduate School of Science, Osaka University, 1-1 Machikaneyama, Toyonaka 560-0043, Japan, [5]Department of Cardiovascular Medicine, Graduate School of Medical Sciences, Kyushu University, 3-1-1 Maidashi, Higashi-ku, Fukuoka 812-8582, Japan, [6]Department of Internal Medicine Kitakyushu City Yahata Hospital, 2-6-2 Ogura, Yahatahigashi-ku, Kitakyushu 805-8534, Japan and [7]Department of Endocrinology and Metabolism, Fukuoka Children's Hospital, 5-1-1 Kashiiteriha, Higashi-ku, Fukuoka 813-0017, Japan

Received November 07, 2022; Revised June 22, 2023; Editorial Decision June 23, 2023; Accepted June 28, 2023

ABSTRACT

The 3243A > G in mtDNA is a representative mutation in mitochondrial diseases. Mitochondrial protein synthesis is impaired due to decoding disorder caused by severe reduction of 5-taurinomethyluridine (τm^5U) modification of the mutant mt-tRNA$^{Leu(UUR)}$ bearing 3243A > G mutation. The 3243A > G heteroplasmy in peripheral blood reportedly decreases exponentially with age. Here, we found three cases with mild respiratory symptoms despite bearing high rate of 3243A > G mutation (>90%) in blood mtDNA. These patients had the 3290T > C haplotypic mutation in addition to 3243A > G pathogenic mutation in mt-tRNA$^{Leu(UUR)}$ gene. We generated cybrid cells of these cases to examine the effects of the 3290T > C mutation on mitochondrial function and found that 3290T > C mutation improved mitochondrial translation, formation of respiratory chain complex, and oxygen consumption rate of pathogenic cells associated with 3243A > G mutation. We measured τm^5U frequency of mt-tRNA$^{Leu(UUR)}$ with 3243A > G mutation in the cybrids by a primer extension method assisted with chemical derivatization of τm^5U, showing that hypomodification of τm^5U was significantly restored by the 3290T > C haplotypic mutation. We concluded that the 3290T > C is a haplotypic mutation that suppresses respiratory deficiency of mitochondrial disease by restoring hypomodified τm^5U in mt-tRNA$^{Leu(UUR)}$ with 3243A > G mutation, implying a potential therapeutic measure for mitochondrial disease associated with pathogenic mutations in mt-tRNAs.

GRAPHICAL ABSTRACT

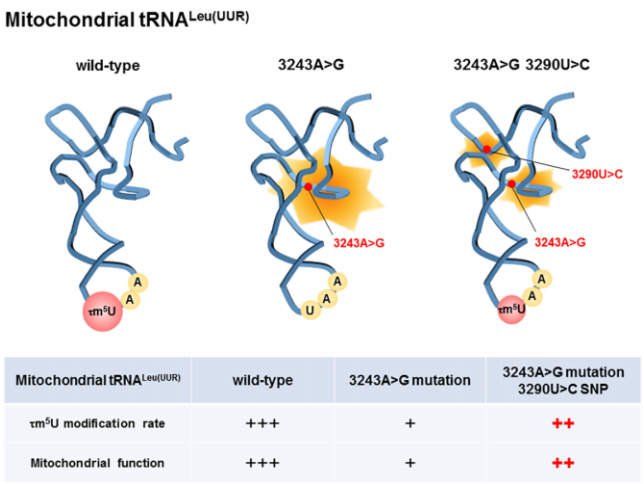

Mitochondrial tRNA$^{Leu(UUR)}$	wild-type	3243A>G mutation	3243A>G mutation 3290U>C SNP
τm^5U modification rate	+++	+	++
Mitochondrial function	+++	+	++

*To whom correspondence should be addressed. Tel: +81 92 642 5750; Fax: +81 92 642 5772; Email: uchiumi.takeshi.008@m.med.kyushu-u.ac.jp

INTRODUCTION

Mitochondrial dysfunction caused by mutations in mitochondrial DNA (mtDNA) or nuclear DNA can lead to the development of various diseases. Point mutations in the genes encoding mt tRNAs are frequently reported as causative mutations in mitochondrial diseases (1). The 3243A > G mutation located in mt $tRNA^{Leu(UUR)}$ gene has been reported in more than 80% of patients with mitochondrial myopathy, encephalopathy, lactic acidosis, and stroke-like episodes (MELAS), one of the major clinical subgroups of the mitochondrial encephalomyopathies. This 3243A > G mutation has been found not only in MELAS patients but also in patients with maternally inherited diabetes and deafness (MIDD), chronic progressive external ophthalmoplegia (CPEO), and cardiomyopathy (2,3). In the adult form with late onset of MELAS with stroke-like symptoms, many patients have already developed diabetes and deafness at the time of onset (4). Sharma et al. showed that many metabolites such as lactate, alanine and α-hydroxybutyrate were increased in patient with MIDD (m.3243A > G) and more elevated in patients with MELAS (m.3243A > G). These biomarkers were correlate strongly with established measures of severity of mitochondrial disease (5).

Mt $tRNA^{Leu(UUR)}$ is responsible for decoding UUR (R = A or G) leucine codon, and the taurine-containing modified uridine (τm^5U; 5-taurinomethyluridine) in the anticodon plays an important role in accurate and efficient translation (6). However, mt $tRNA^{Leu(UUR)}$ with MELAS 3243A > G mutation lacks the τm^5U modification, resulting in translation defects at the UUG codon (6). Decoding disorders due to deficient τm^5U modification reduced oxidative phosphorylation. This molecular mechanism is supposed to be a major cause of mitochondrial dysfunction (6,7). Thirteen proteins encoded by mtDNA are essential subunits of the respiratory chain complex, seven of which are present in complex I. Since ND6, a subunit of complex I, has the highest usage of UUG codons, translation of ND6 is severely affected by a reduction of τm^5U modification on the MELAS mt $tRNA^{Leu(UUR)}$, leading to reduced activity of complex I as the major biochemical symptom of MELAS (6,8). In addition, the 3243A > G mutation in mt $tRNA^{Leu(UUR)}$ causes a remarkable change in the L-shaped tertiary structure, resulting in decreased stability, decreased aminoacylation, and impaired transcriptional termination (6,9,10). Many functional analyses of mitochondria with the 3243A > G mutation have been performed using cybrid cells and myoblasts with mitochondria from MELAS and MIDD patients. These analyses have reported decreases in mitochondrial protein synthesis, oxygen consumption rate, respiratory chain enzyme activity, and mt $tRNA^{Leu(UUR)}$ level. However, the detailed molecular mechanisms behind the mitochondrial dysfunction remain to be elucidated (6,7,9,11–15).

Loss of τm^5U modification was found in mt $tRNA^{Leu(UUR)}$ with one of five different point mutations (3243A > G, 3244G > A, 3258T > C, 3271T > C and 3291T > C) derived from patients presenting clinical features of MELAS (16). In contrast, mt $tRNA^{Leu(UUR)}$ with one of four different mutations (3242G > A, 3250T > C, 3254C > T and 3280A > G) derived from patients showing non-MELAS symptoms retained τm^5U modifications (16). Therefore, loss of τm^5U modification in mt $tRNA^{Leu(UUR)}$ seems to be associated with the clinical features of MELAS. Since τm^5U formation in mt $tRNA^{Leu(UUR)}$ is catalyzed by an enzyme complex, MTO1 and GTPBP3 (17), it is likely that the MELAS mutations prevent τm^5U-modifying enzyme from recognition of mt $tRNA^{Leu(UUR)}$ (16,18–22).

The mtDNAs with 3243A > G mutation are present in cells as a heteroplasmic mixture with the wild type mtDNA, and tissue-specific presentations appear when mutated mtDNA crosses a threshold regarding the rate of 3243A > G heteroplasmy. In non-meristematic tissue such as skeletal muscle, mutated mtDNA tends to accumulate and the mutation rate in each tissue correlates with age and disease severity. Meanwhile, 3243A > G heteroplasmy has been reported to decrease exponentially with age in peripheral blood because hematopoietic stem cells with 3243A > G mutation are selectively eliminated (23,24). However, some case reports have indicated that patients with the 3290T > C single-nucleotide polymorphism (SNP) in addition to the 3243A > G mutation in mt $tRNA^{Leu(UUR)}$ show clinical phenotypes not typical of 3243A > G mutation despite a high rate of 3243A > G heteroplasmy in peripheral blood (25,26). Liu et al. reported that patients with respiratory symptoms and asymptomatic families have high 3243A > G heteroplasmy in peripheral blood, but the mechanism behind this has not been elucidated (26).

We found four cases from two families that were asymptomatic or had mild disease despite high frequency of 3243A > G heteroplasmy in peripheral blood. In these cases, the 3290T > C haplotypic mutation in addition to the 3243A > G mutation was detected in mt $tRNA^{Leu(UUR)}$ gene. This haplotypic mutation has been rarely reported in cases with 3243A > G mutation. We here showed that 3290T > C haplotypic mutation improved mitochondrial protein synthesis, formation of respiratory chain complex, and oxygen consumption rate of cybrid cells with 3243A > G mutation. We also observed partial restoration of the τm^5U modification of mt $tRNA^{Leu(UUR)}$ bearing both 3243A > G and 3290T > C haplotypic mutations. There findings contribute to our understanding of the molecular pathogenesis and potential treatment of MELAS.

MATERIALS AND METHODS

Antibodies

The antibodies used in this study are listed in Supplementary Table S1.

Cell culture

Cybrid cell lines 2SA and 2SD had been generated earlier by fusing mtDNA-less 143B osteosarcoma ρ0 cells with enucleated myoblasts from a MELAS patient with the heteroplasmic 3243A > G mutation and isolating cybrid clones, as described previously (13). The 2SA cells containing only normal mtDNA and 2SD cells possessing 94% 3243A > G-mutated mtDNA were obtained;

then, the rate of mutated mtDNA of 2SD cells was increased by cloning. Cybrid cell line 2KD was generated by fusing 143Bρ0 cells with platelets from a patient with the heteroplasmic 3243A > G mutation and homoplasmic 3290T > C SNP and isolating two cybrid clones (2KD-1, 2KD-2), via a previously reported procedure (27). This study was approved by the Ethical Review Board of the Graduate School of Medical Science, Kyushu University. Informed consent was obtained from all participants. 2SA and 2KD cells were cultured in Dulbecco's modified Eagle's medium (DMEM) (1000 mg/l glucose) (Sigma-Aldrich, St. Louis, MO, D6046) supplemented with 10% FBS at 37°C in a humidified atmosphere with 5% CO_2. 2SD and 143Bρ0 cells were cultured in DMEM (4500 mg/l glucose) (Nacalai, Kyoto, Japan, 16972-45) supplemented with 100 μg/ml pyruvate, 50 μg/ml uridine, and 10% FBS at 37°C in a humidified atmosphere with 5% CO_2.

mtDNA sequencing

Total DNA was extracted using the QIAamp DNA Blood Mini Kit (Qiagen, Hilden, Germany, 51104) in plasma, and using Nucleospin Tissue (Takara Bio Inc., Shiga, Japan, 740952) from cybrid cells derived from the patients with the 3243A > G mutation and 3290T > C SNP. Total DNA was then subjected to PCR analysis with LA Taq (Takara, RR002A) and T100TM PCR Thermal Cycler Dice Gradient (Takara). The generation of PCR products was confirmed by electrophoresis, and PCR products were purified using Illustra MicroSpin Columns (GE Healthcare Systems, Chicago, IL, 28917920). The sequencing reaction was performed with Big Dye Terminator v3.1 Cycle Sequencing Kit (Thermo Fisher Scientific, Waltham, MA, 4336917), after which mtDNA sequencing was performed with 3500xL Genetics Analyzer (Thermo Fisher Scientific). Data processing was carried out using CLC Genomics Workbench6 (Qiagen).

Analysis of 3243A > G mutation rate

The 3243A > G heteroplasmy of the 2SA, 2SD and 2KD cells were analyzed by the Droplet Digital PCR assay. The ddPCR mixture consisted of total DNA, 2× ddPCR Supermix for Probes (no dUTP) (Bio-Rad, Hercules, CA, 1863024), wild-type and mutant allele-specific probes, primer mixtures for the target gene, and the 2U/reaction Alu I enzyme (New England Biolabs, Ipswich, MA, R01375). All primers and probes were obtained from Bio-Rad. Sequences and other information are available at www.bio-rad.com with assay ID dHsaMDS556387941. Droplets were generated with the Bio-Rad QX200 system (Bio-Rad), in accordance with the manufacturer's instructions. The reactions were then subjected to PCR analysis with Thermal Cycler (Applied Biosystems, Waltham, MA). The number of fluorescence-positive droplets was analyzed using QX200 Droplet Reader (Bio-Rad). A two-color detection system (set to detect FAM and HEX) was used to analyze each droplet separately. The fluorescent droplets were counted and absolute quantification of the copy number of wild type and mutant at m.3243 was performed using QuantaSoft software 1.7 (Bio-Rad). The 3243A > G heteroplasmy was calculated as follows.

$$3243\text{A} > \text{G heteroplasmy} = \frac{\text{copy number in mutated mtDNA}}{\text{sum of the copy number in normal mtDNA and mutated mtDNA}} \times 100$$

Growth curve analysis

To determine cell proliferation, 2SA, 2SD, 2KD-1, 2KD-2 and 143Bρ0 cells (1×10^4) were seeded in triplicate in 12-well plates and cultured under high-glucose (4500 mg/l glucose DMEM supplemented with 100 μg/ml pyruvate, 50 μg/ml uridine, 10% FBS) or high-galactose (no glucose (Nacalai, 09891-25) supplemented with 1800 mg/l galactose, 10% FBS) conditions. Cells were trypsinized and counted daily for up to 5 days using a Coulter Counter (Beckman Coulter, Brea, CA). Half proportion of each medium was refreshed on Day 3.

Immunoblotting

Briefly, 2SA, 2SD, 2KD-1, 2KD-2 and 143Bρ0 cells were lysed with lysis buffer [20 mM Tris–HCl, pH 7.5, 150 mM NaCl, 2 mM EDTA, 1% NP-40, 0.1% SDS, protease inhibitor cocktail (Wako, Osaka, Japan, 161-26023)] and homogenized by sonication, as described elsewhere (28). Samples containing 5 μg of protein were separated by SDS-PAGE, and then subjected to immunoblotting with antibodies against ND1, NDUFB8, NDUFA9, SDHA, UQCRC1, COX I, COX II, ATP5A1, ATP6 and ATP8.

Real-time PCR analysis

Real-time PCR analysis was performed with reference to the previous method (29). Total RNA was extracted using the RNeasy® Mini Kit (Qiagen, 74104). The RNase-Free DNase Set (Qiagen, 79254) was used to remove DNA during RNA purification, and the RNA was quantified using Nano Drop ND-1000 Spectrophotometer (Thermo Fisher Scientific). The cDNA was synthesized with 500 ng of total RNA, 5 μM of random 6-mers, 2.5 μM of oligo dT primers, and the PrimeScript™ RT Reagent Kit (Takara, RR037A) for a final volume of 10 μl. The reverse transcription reaction was conducted using a BLOCK INCUBATOR (ASTEC, Fukuoka, Japan, BI-526) under the following conditions: reverse transcription for 15 min at 37°C and enzyme inactivation for 5 s at 85°C. The real-time PCR mixture consisted of 8 ng cDNA, TB Green Premix Ex Taq™ II (Takara, RR820A), and primer mixtures at a concentration of 0.8 μM for target gene for a final volume of 20 μl. The PCR analysis was conducted using StepOnePlus Real-Time PCR System (Applied Biosystems) under the following conditions: activation of the enzyme at 95°C for 1 min, then 40 cycles of a two-step protocol consisting of incubation at 95°C for 15 s followed by combined annealing/extension at 60°C for 1 min. The expression level of each mRNA

was normalized to the level of 18S ribosomal RNA obtained from the corresponding reverse transcription product. All primers were purchased from Eurofins (Luxembourg). Primer sequences are listed in Supplementary Table S2.

Oxygen consumption assay

Oxygen consumption rate (OCR) was measured as previously described (30). The 2SA, 2SD, 2KD-2 and 143Bρ0 cells (1×10^5) were seeded in XF24-well microplates (Seahorse Bioscience, North Billerica, MA). Oxygen concentrations were measured at 37°C with an uncoupler (FCCP) and inhibitors (oligomycin, rotenone, and antimycin A) using XF^{e}24 Extracellular Flux Analyzer (Seahorse Bioscience), in accordance with a standard protocol. Oxygen consumption rate is presented as the mean ± SD, in the unit of nmol O_2 consumed per minute per cell.

Pulse-labeling of mitochondrial translation products

Mitochondrial translation products were pulse-labeled *in vitro* with [^{35}S]-methionine and [^{35}S]-cysteine. The 2SA, 2SD and 2KD-2 cells were incubated for 10 min in 100 μg/ml emetine and 200 μg/ml cycloheximide prior to labeling for 60 min. After incubation, labeled cells were washed with PBS and then lysed in lysis buffer (10 mM Tris–HCl, pH 7.5, 1 mM EDTA, 8 M urea, 1% SDS). Total cellular protein (10 μg/lane) was subjected to 15–20% SDS-PAGE for 3 h at 180 V. The gels were stained with Coomassie Brilliant Blue and dried. The gels were measured using a BAS2500 bio-imaging analyzer (Fujifilm, Tokyo, Japan).

BN-PAGE and immunoblotting

The formation of complexes I to V was evaluated by performing electrophoresis while maintaining the complex structure. Each step was carried out at 4°C or on ice. The 2SA, 2SD and 2KD-2 cells (2×10^7) were homogenized with a Potter-Elvehjem homogenizer in 1 ml of homogenizing buffer [20 mM HEPES–KOH, pH 7.4, 0.25 M sucrose, 1 mM EDTA, protease inhibitor cocktail (Wako)] and centrifuged at 3000 rpm for 15 min. The supernatant was centrifuged at 10 000 rpm for 25 min, and the mitochondrial pellet was lysed with solubilization buffer (50 mM Bis–Tris/HCl, pH 7.0, 1.5 M 6-aminocaproic acid) and 1/10 volume of 10% *n*-dodecyl-β-D-maltoside (Wako, 341-06161) solution. The sample was centrifuged at 18 000 g for 20 min and 1/20 volume of sample buffer (50 mM Bis–Tris/HCl, pH 7.0, 0.75 M 6-aminocaproic acid, 5% CBB G-250) and glycerol was added to the supernatant. Each sample (5 μg of mitochondrial protein) was then loaded onto a 3–12% BN-PAGE gradient gel (Invitrogen, Carlsbad, CA). Electrophoresis was performed with cathode buffer in the upper buffer chamber and anode buffer in the lower buffer chamber using a CROSSPOWER 3500 (ATTO, Tokyo, Japan). The electrophoresis was carried out at 4°C and 90 V for 30 min and then raised to 6 mA for 2.5 h. When the front was about halfway across the gel, cathode buffer A was substituted by cathode buffer B. Cathode buffer A consisted of 50 mM Tricine, 15 mM Bis–Tris/HCl, pH 7.0, and 0.02% (w/v) CBB G-250; cathode buffer B consisted of 50 mM Tricine, 15 mM Bis–Tris/HCl, pH 7.0, and 0.002% (w/v) CBB G-250; and the anode buffer consisted of 50 mM Tricine and 15 mM Bis–Tris/HCl, pH 7.0. The separated proteins were transferred electrophoretically onto a PVDF membrane with NuPAGE Transfer buffer [25 mM Bicine, 25 mM Bis–Tris, pH 7.2, 1 mM EDTA] and immunoblotted with antibodies against ND1, NDUFB8, SDHA, UQCRC1, COX I, ATP5A1 and ATP6.

Immunofluorescence imaging of mitochondria

Immunofluorescence was carried out in accordance with established techniques. Briefly, 2SA, 2SD and 2KD-2 cells were incubated in the presence of 100 nM MitoTracker™ Red CMXRos (Invitrogen, M7512) for 20 min. Cells were fixed and permeabilized, and then incubated in the presence of 4′,6-diamidino-2-phenylindole (DAPI) (Fujifilm, 340-7971) for 45 min. Glass slides were mounted using Superfrost (Matsunami, Osaka, Japan). Fluorescence images were obtained using a confocal laser microscope (KEYENCE, Osaka, Japan).

RNA preparation for primer extension method and northern blotting

Total RNA was extracted from each cell using custom-made RNA isolation reagent [40%(w/v) phenol, 1%(v/v) ethylene glycol, 2 M guanidine thiocyanate, 0.1%(w/v) (6.9 μM) 8-quinolinol, 20 mM tri-sodium citrate·2H_2O, 0.1 M NaOAc (pH 4.5), 0.1% (v/v) Triton X-100, 0.2% (w/v) *N*-lauroylsarcosine sodium salt, 50 mM salicylic acid, 10 μM Aluminon, 0.0001% (w/v) Bromophenol Blue]. The solution was centrifuged and chloroform was added to the aqueous phase to a concentration of 20%. After vortexing and centrifugation, the RNAs were precipitated from the aqueous phase with 2-propanol.

Primer extension method

To quantify τm^{5}U frequency in mt tRNA$^{Leu(UUR)}$, we employed a primer extension method assisted by chemical derivatization of τm^{5}U (31). The total tRNA fraction was purified by electrophoresis on a 10% polyacrylamide gel containing 7 M urea and gel extraction. Then, CMC [*N*-cyclohexyl-*N*'-β-(4-methylmorpholinium) ethylcarbodiimide] derivatization of mt tRNA$^{Leu(UUR)}$ in the total RNA fraction was performed as described previously (6,32). The CMC-derivatized mt tRNA$^{Leu(UUR)}$ was subjected to a reverse-transcription reaction with 5′-[^{32}P]-labeled primer for mt tRNA$^{Leu(UUR)}$ (5′-ACCTCTGACTGTAAAG-3′) and SuperScript III Reverse Transcriptase (Invitrogen) in buffer containing 1 × FS buffer (Invitrogen), 3.75 mM $MgCl_2$, 0.0375 mM each of dATP and dTTP, and 0.075 mM ddGTP at 55°C for 1 h. The cDNAs were subjected to 20% PAGE with 7 M urea (20×20 cm^2, 0.35 mm). The gel was exposed to an imaging plate and visualized using an FLA-7000 imaging analyzer (Fujifilm).

Northern blotting

Northern blotting analysis of mt tRNA$^{Leu(UUR)}$ was conducted essentially as described previously (33). Total

RNA (3 μg) from cultured cells was dissolved in 10% PAGE containing 7 M urea and stained with ethidium bromide before blotting onto a nylon membrane (Amersham Hybond N+; GE Healthcare Systems). A synthetic DNA probe for mt tRNA$^{Leu(UUR)}$ was 5′-labeled with [γ-^{32}P]ATP (PerkinElmer, Inc., Waltham, MA) by T4 Polynucleotide Kinase (Toyobo, Osaka, Japan). The following two types of probes were used: probe 1 (5′-TGTTAAGAAGAGGAATTGAACCTCTGACTG-3′) for comparing 2SA cells with 2SD cells, and probe 2 (5′-TTTTATGCGATTACCGGGCCCTGCCATCTT-3′) for comparing 2SD cells with 2KD cells. The radioactivity on the membrane was visualized by exposing the membrane to an imaging plate and analyzed using an FLA-7000 imaging analyzer (Fujifilm). The 5S rRNA was detected by ethidium bromide staining.

In vitro transcription and tRNA purification

Three types of mt tRNA$^{Leu(UUR)}$ sequences (wild-type, 3243A > G mutation, 3243A > G mutation and 3290T > C SNP) were amplified using 2SA, 2SD, and 2KD genomic DNA and primers with *Aat* II and *Sal* I sequences at each end (Supplementary Table S2). The PCR analysis was conducted using PCR Thermal Cycler Dice TP-600 (Takara) and KOD -plus- (Toyobo, KOD-201) under the following conditions: pre denature at 94°C for 2 min, then 30 cycles of a three-step protocol consisting of denature at 94°C for 15 s, annealing at 55°C for 30 s, and extension at 68°C for 30 s. Three types of mt tRNA$^{Leu(UUR)}$ sequences were cloned by inserting into pGEM®-T Easy Vector (Promega, Madison, WI, A1360). Each plasmid was extracted using the Wizard® Plus SV Minipreps DNA Purification Systems (Promega, A1460) and linearized by *Sal* I restriction enzyme digestion. Then, *in vitro* run-off transcription was performaed by using a Riboprobe®*in vitro* Transcription Systems (Promega, P1440). The transcription reaction was performed at 37°C for 1 h in Transcription Optimized 5 × Buffer, 10 mM DTT, 20 u Recombinant RNasin® Ribonuclease Inhibitor, 2.5 mM nucleotides (rATP, rGTP, rCTP and rUTP), using 200 μg/ml of the plasmid and 15 u T7 RNA Polymerase. Subsequently, *in vitro* transcript was purified and DNase treated using a RNA Clean and Concentrator-5 kit (Zymo Research, Irvine, CA, R1013). The RNA was eluted in a buffer containing 20 mM Tris–HCl, pH 7.5, and 50 mM NaCl, and melt curve analysis and polyacrylamide gel electrophoresis were performed.

Melt curve analysis

To determine the differences of mt tRNA$^{Leu(UUR)}$ structures, a melt curve analysis was performed by using 1:10 000 SYBR Green I Nucleic Acid Gel Stain (Thermo Fisher Scientific, S7563) with reference to the previous method (34). First, a 10 × SYBR Green I Buffer was prepared in 100 mM Tris–HCl, pH 7.5, 20 mM $MgCl_2$, 1.5% (v/v) Triton X-100 and 1.5 M NaCl by diluting the original dye 1000-fold. To prepare samples for the melt curve analysis, purified tRNA samples were incubated at 65°C for 5 min and then at room temperature for 45 min. For RNase A treatment of mt tRNA$^{Leu(UUR)}$, wild-type tRNA$^{Leu(UUR)}$ was incubated with 2 μg/μl RNase A (Wako, 182-01493) at 37°C for 5 min. Then, tRNA samples (wild-type tRNA$^{Leu(UUR)}$, tRNA$^{Leu(UUR)}$ with 3243A > G mutation, tRNA$^{Leu(UUR)}$ with 3243A > G mutation and 3290T > C SNP, RNase A-treated wild-type tRNA$^{Leu(UUR)}$, and no RNA) were diluted in the 1 × SYBR Green I Buffer. The melt curve analysis was conducted using a 20 μl sample volume on the StepOnePlus Real-Time PCR System (Applied Biosystems) in triplicate with a temperature gradient of 0.5°C /s from 50 to 95°C.

Aminoacylation assay

The *in vivo* aminoacylation status of mt tRNA$^{Leu(UUR)}$ was analyzed by acid-urea northern blotting (35) with slight modifications. Total RNA was extracted under acidic conditions at low temperature as described previously (36). Three to ten μg of total RNA was resolved by 7.5% PAGE containing 7 M urea and 0.1 M NaOAc (pH 5.2) at 4°C overnight, blotted onto a nylon membrane, dried, and crosslinked by UV as described above. The DNA probes for mt tRNA$^{Leu(UUR)}$ (5′-TGTTAAGAAGAGGAATTGAACCTCTGACTG-3′) were 5′-labeled with ^{32}P, and northern blotting was performed as described above.

Metabolomics

Blood samples were collected from three individuals in each of the following groups: patients with 3243A > G and 3290T > C, MIDD patients with 3243A > G, and controls, after fasting for more than 5 h (Supplementary Table S3). Plasma samples were analyzed using LCMS-8060 (Shimadzu, Kyoto, Japan), as described previously (37). Data processing was carried out using MetaboAnalyst (www.metaboanalyst.ca).

RESULTS

Patients with the 3243A > G mutation with 3290T > C SNP

The 3243A > G mutation, a typical causative mutation of mitochondrial disease, causes hearing loss, diabetes, and MELAS-like symptoms (Figure 1A). As for 3243A > G heteroplasmy, it decreases with age in peripheral blood. In the 44 cases analyzed in our laboratory, the rate of 3243A > G heteroplasmy in peripheral blood decreased exponentially with age (Figure 1B). However, we experienced four cases in two families that deviated significantly from this relationship between age and 3243A > G heteroplasmy, and they were asymptomatic or had mild disease despite markedly high rates of heteroplasmy (Figure 1B and C). Three patients (#1–1, #1–2 and #2–2) with mild disease had no hearing loss, diabetes, or muscle symptoms despite the 3243A > G heteroplasmy being over 90% in peripheral blood, and they shared respiratory failure in common, which is rarely reported in patients with 3243A > G mutation (Figure 1D). One patient (#2–1) was asymptomatic despite a 70.6% rate of heteroplasmy in peripheral blood. We confirmed the presence of the 3243A > G mutation and 3290T > C SNP in mt tRNA$^{Leu(UUR)}$ in only these four cases by analyzing the full-length mtDNA sequence

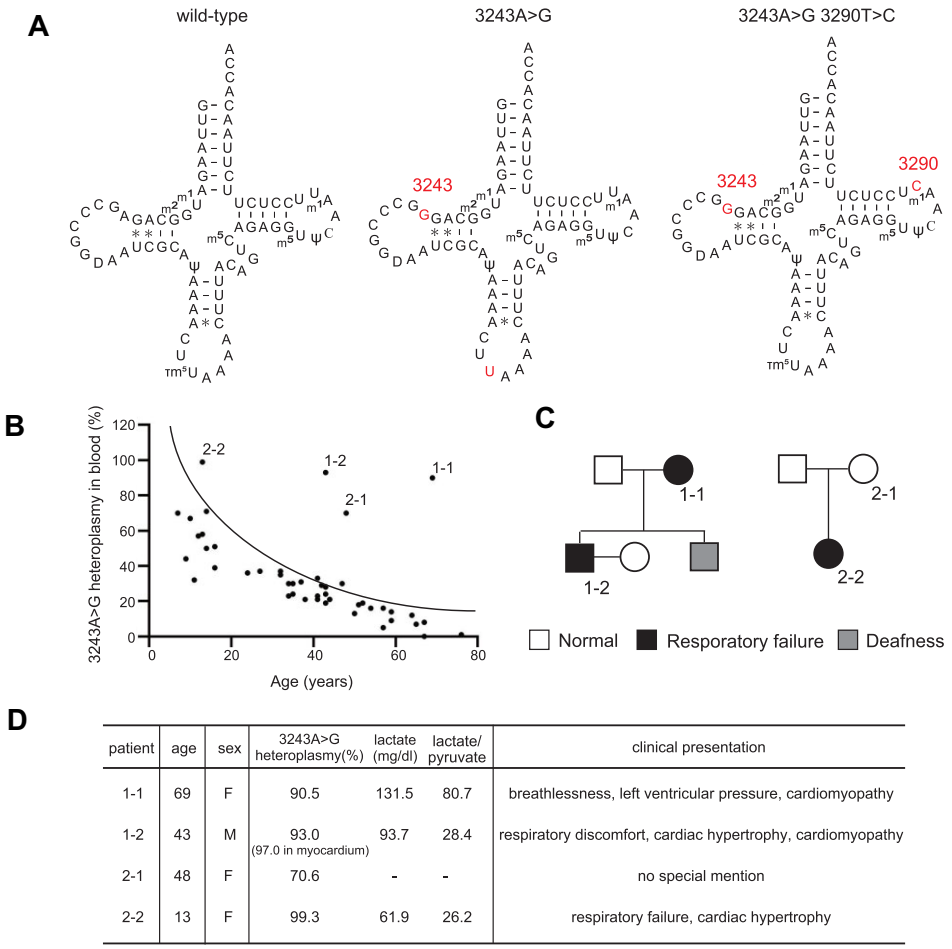

D

patient	age	sex	3243A>G heteroplasmy(%)	lactate (mg/dl)	lactate/ pyruvate	clinical presentation
1-1	69	F	90.5	131.5	80.7	breathlessness, left ventricular pressure, cardiomyopathy
1-2	43	M	93.0 (97.0 in myocardium)	93.7	28.4	respiratory discomfort, cardiac hypertrophy, cardiomyopathy
2-1	48	F	70.6	-	-	no special mention
2-2	13	F	99.3	61.9	26.2	respiratory failure, cardiac hypertrophy

Figure 1. Clinical information on patients with the 3243A > G mutation with 3290T > C SNP. (**A**) Cloverleaf structures of human mt tRNA$^{Leu(UUR)}$ with modified bases. Left panel, wild-type tRNA; central panel, tRNA with 3243A > G mutation; right panel, tRNA with 3243A > G mutation and 3290T > C SNP. (**B**) The levels of 3243A > G heteroplasmy of mtDNA in peripheral blood derived from 48 patients. (**C**) Pedigrees of patients of two families. #1–1, #1–2, #2–1 and #2–2 have 3243A > G mutation with 3290T > C SNP. Black shows respiratory failure patients. Diagonal square shows deaf patients, for whom sequencing was not performed. (**D**) Disease features of four patients having the 3243A > G mutation and 3290T > C SNP.

(Supplementary Figure S1). This suggests that the presence of the 3290T > C SNP is related to differences in clinical phenotype.

Patient #1–2 has a history of left ventricular hypertrophy, sleep apnea, respiratory acidosis, and type II respiratory failure, and showed improvements in symptoms after the introduction of non-invasive positive pressure ventilation. Although there was no indication of symptoms typical of mitochondrial disease, such as loss of limb muscle strength, cranial neurological shedding, or heart failure, the treatment of mitochondrial cardiomyopathy was implemented. The rate of 3243A > G heteroplasmy was remarkably high, at 93.0% in peripheral blood and 97.0% in myocardium. Blood tests showed a high lactate level and high lactate/pyruvate ratio of 93.7 mg/dl and 28.4, respectively (Figure 1D).

Against the above background, we generated cybrid cells named 2KD cells using platelets from patient #1–2 and 143B osteosarcoma ρ0 cells to investigate whether the presence of the 3290T > C SNP in addition to the 3243A > G mutation improves the mitochondrial damage associated with the latter mutation. All six clones of cybrid 2KD cell lines had 99.8% or higher rate of 3243A > G heteroplasmy (Supplementary Table S4), and the presence of 3290T > C SNP was confirmed in the two clones of 2KD-1 and 2KD-2 (Supplementary Figure S2).

In addition, mtDNA sequencing analysis confirmed that the hypervariable D-loop region of the 2KD-1 and 2KD-2 clones had the same sequence as that of the blood samples from patient #1–2. We used wild-type 2SA cells and 3243A > G 2SD cells as controls, the rates of 3243A > G heteroplasmy of which were 0.02% and 99.9%, respectively (Supplementary Table S4). The mtDNA copy number was 192 copies/cell in the 2SA cells and 258 copies/cell in the 2SD cells. The 2KD cells showed a copy number range of 180–270 copies/cell.

Mitochondrial dysfunction is relatively mild in 2KD cells with the 3243A > G mutation with 3290T > C SNP

We decided to evaluate mitochondrial function in the 2KD cells with the 3243A > G mutation with the 3290T > C SNP. Comparative analysis was performed using wild-type 2SA cells and 3243A > G 2SD cells. First, to examine cell

proliferation, 2SA, 2SD, 2KD-1, 2KD-2 and 143Bρ0 cells were cultured under high-glucose and high-galactose conditions for 5 days. The high glucose conditions resulted in an exponential increase in the numbers of all five cells, including 2SA cells (Figure 2A). Under the high-galactose conditions, in which mitochondrial oxidative phosphorylation is relied upon for energy production, 2SD and ρ0 cells showed no growth. In contrast, two clones of the 2KD cells showed proliferation following the 2SA cells (Figure 2A). This suggests that 2SD cells with impaired mitochondrial function and 143Bρ0 cells without mtDNA cannot proliferate in a mitochondrially dependent manner, while 2KD cells can produce energy in a manner dependent on mitochondria.

Interactions between mitochondria and the endoplasmic reticulum play an important role in the regulation of mitochondrial function and dynamics (38,39). The expression of genes related to the endoplasmic reticulum (ER) stress response, integrated stress response, and acting as biomarkers of mitochondrial disease is elevated in response to mitochondrial dysfunction. Therefore, we evaluated the degree of mitochondrial dysfunction using ER stress response markers such as *CHOP*, *GADD34*, *Trib3* and *ATF4* and a biomarker of mitochondrial disease, *GDF15*. Compared with the levels in the 2SA cells with normal mitochondrial function, the expression of all genes was significantly elevated in the 2SD cells (Figure 2B). Gene expression of the four ER stress response markers in the two clones of 2KD cells was comparable to that in the 2SA cells (Figure 2B). Expression of the *GDF15* gene in the 2KD cells was not as decreased as in the 2SA cells, but was lower than in the 2SD cells (Figure 2B). This suggests that mitochondrial damage is suppressed in the 2KD cells compared to the 2SD cells.

Next, oxygen consumption was measured to assess mitochondrial oxidative phosphorylation. In the 2SD cells, oxygen consumption was markedly reduced compared with that in the 2SA cells. However, oxygen consumption of the 2KD cells was intermediate between the levels in 2SA and 2SD cells in terms of both basal and maximal respiratory capacity and recovered to approximately half that of the 2SA cells (Figure 2C and Supplementary Figure S3). This suggests that oxidative phosphorylation in the 2KD cells was improved over that in the 2SD cells, but not as much as in the 2SA cells.

Mitochondrial morphological dynamics is associated with the regulation of cellular function and disease, and fragmented mitochondria are observed in cells in cases of mitochondrial disorders (40–43). Therefore, immunostaining was performed to evaluate mitochondrial morphology. When cells were classified by the mitochondrial morphology, >70% of the 2SA cells were classified as filament (Figure 2D). Meanwhile, more than 90% of the 2SD cells were classified as fragmentation, while no cells consisting only of filament-like mitochondria were found (Figure 2D). In the 2KD cells, around 60% of cells were classified as fragmentation and around 20% as filament (Figure 2D). Compared with the 2SD cells, 2KD cells showed a decrease in fragmented mitochondria and an increase in filamentous ones. These results suggest that mitochondrial function is improved in the 2KD cells compared with that in the 2SD cells.

Mitochondrial translation was partially improved in the 2KD cells with 3243A > G mutation and 3290T > C SNP

In 3243A > G cybrid cells (2SD cells), the synthesis of mtDNA encoded proteins is downregulated due to the decrease in τm^5U modification in mt $tRNA^{Leu(UUR)}$ (7). Therefore, we examined the expression of proteins constituting the mitochondrial respiratory chain to assess the mitochondrial translation function in the 2KD cells. The expression of mtDNA encoded proteins was significantly downregulated in the 2SD and 143Bρ0 cells compared with that in the 2SA cells (Figure 3A). In the 2SD and 143Bρ0 cells, the levels of nuclear-encoded proteins such as NDUFB8, NDUFA9, and UQCRC1 were also decreased (Figure 3A). This downregulation may have been accompanied by destabilization of the complex and nuclear-encoded subunits. In contrast, the expression was completely improved in the two clones of 2KD cells (Figure 3A). In addition, the level of SDHA was slightly increased in the 2SD and 143Bρ0 cells (Figure 3A). These results suggest that 2KD cells are capable of synthesizing mtDNA encoded proteins and any deficiency in the expression of proteins consisting of the mitochondrial respiratory chain is completely overcome.

Next, we performed a pulse-labeling assay to comprehensively assess the rates of synthesis of 13 mtDNA encoded proteins. In the cell line we used, 11 subunits showed band changes, but two subunits, ND3 and ND6, had weak bands and were not detectable. In 2SD cells, all proteins were synthesized at lower levels than in 2SA cells, approximately 15–50% of the 2SA cell levels (Figure 3B and Supplementary Figure S4). However, in 2KD cells, most proteins tended to be synthesized at higher ones than in 2SD cells, approximately 50–100% of the 2SA cell levels (Figure 3B and Supplementary Figure S4). In addition, no abnormal bands or translation defects, indicating amino acid misincorporation, were observed. These results indicate that 2KD cells have an increased rate of protein synthesis compared with 2SD cells, but that translational function has not been restored to the same extent as in 2SA cells. This incomplete recovery of the capacity for protein synthesis may have led to a partial recovery of oxygen consumption.

The 2KD cells form an incomplete respiratory chain complex

Despite the complete improvement in the expression of mitochondrial respiratory chain subunits in the 2KD cells, protein synthesis capacity and oxidative phosphorylation were shown to be approximately half those of the 2SA cells (Figures 2C, 3A and B). Therefore, we hypothesized that the formation of the respiratory chain complex is reduced by an imbalance between translation in the mitochondria and proteins derived from the nuclear genome. To examine the ability to form respiratory chain complexes, we evaluated the formation of complexes I–V by blue native PAGE (BN-PAGE). First, immunoblotting of the complex I subunit NDUFB8 detected complex I and a supercomplex ($I + III_2 + IV$) in the 2SA and 2KD cells (Figure 4A). The 2SD cells showed less complex formation as well as the presence of incompletely formed subcomplexes (Figure 4A). Next, we examined the complex formation using ND1 antibody that recognizes a region located inside complex I

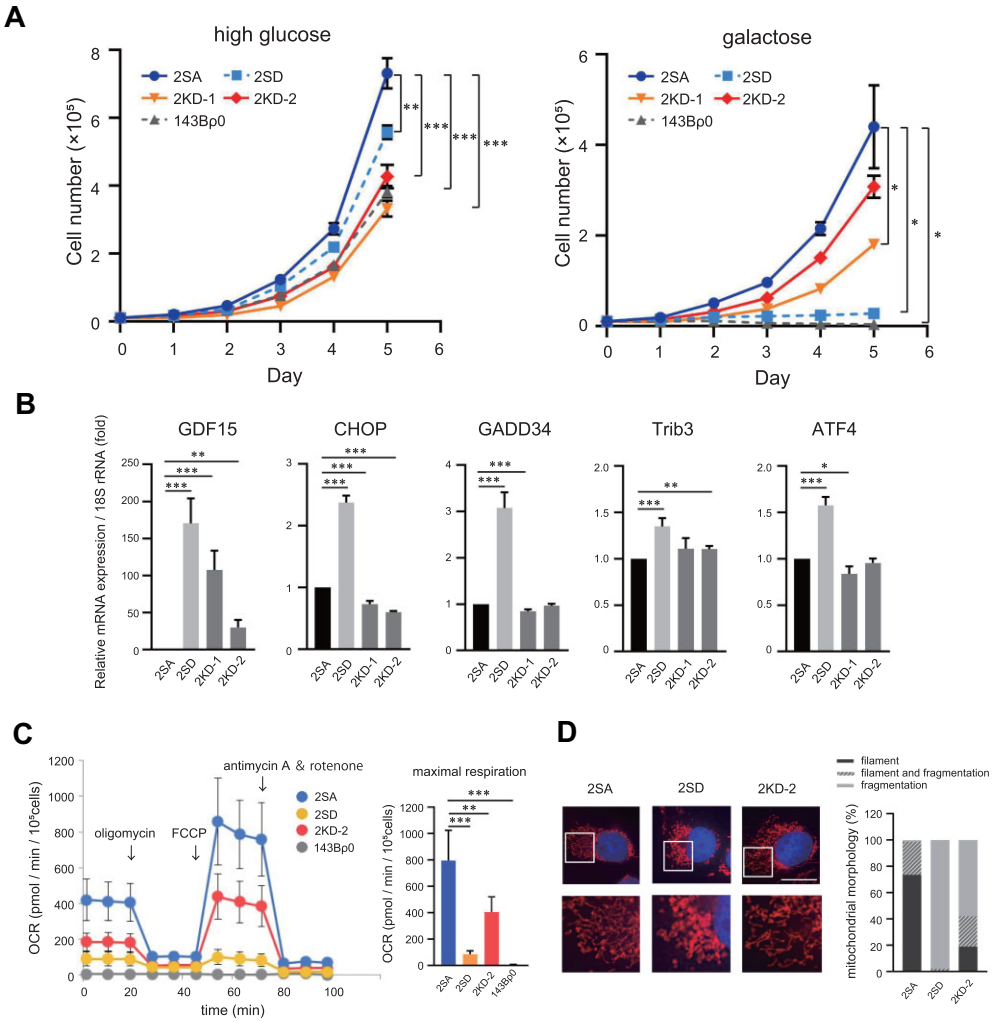

Figure 2. Improvement in oxidative phosphorylation and mitochondrial function in the 2KD cells. (**A**) Cell proliferation monitored in the 2SA, 2SD, 2KD-1, 2KD-2 and 143Bρ0 cells under high-glucose (left panel) and high-galactose (right panel) conditions. The cell number was determined every 24 h for 5 days after seeding. Results are expressed as the mean ± SD of three independent experiments. Student's *t*-test was performed vs. 2SA cells at day 5, $*P < 0.05$, $**P < 0.01$, $***P < 0.001$. (**B**) The mRNA abundance of the ISR-related gene markers, *CHOP*, *GADD34*, *Trib3* and *ATF4*, and a biomarker of mitochondrial disease, *GDF15*, was assessed by RT-qPCR in the 2SA, 2SD, 2KD-1 and 2KD-2 cells. Results are expressed as the mean ± SD of three independent experiments. Student's *t*-test was performed vs. 2SA cells, $*P < 0.05$, $**P < 0.01$, $***P < 0.001$. (**C**) Oxygen consumption in the 2SA, 2SD, 2KD-2 and 143Bρ0 cells. (Left panel) Oligomycin (a complex V inhibitor) reversibly inhibits O_2 consumption, FCCP (an uncoupler of ETC and ATP synthase) allows maximum O_2 consumption, while rotenone (complex I inhibitor) and antimycin A (complex III inhibitor) completely inhibit O_2 consumption. Results are expressed as the mean ± SD of five independent experiments. (Right panel) Maximal respiration in the 2SA, 2SD, 2KD-2 and 143Bρ0 cells. Results are expressed as the mean ± SD of five independent experiments. Student's *t*-test was performed vs. 2SA cells, $**P < 0.01$, $***P < 0.001$. (**D**) (Left panel) Immunofluorescence staining of MitoTracker™ Red CMXRos in the 2SA, 2SD and 2KD-2 cells. Nuclei were stained with 4′,6-diamidino-2-phenylindole (DAPI). Scale bar: 20 μm. (Right panel) Mitochondrial morphology of each cell was classified as follows: filament, more than 80% were long and higher interconnected; fragmentation, >80% were small and round; filament and fragmentation, mixture of shorter filaments and round. The mitochondrial morphology rates were determined as percentages of the total number of cells counted (∼100 cells).

(Figure 4B) and found that complex I and the supercomplex were detected by this antibody in the 2KD cells, but only slightly in the 2SA cells (Figure 4B, left panel). This may indicate that the complex I structure in the 2KD cells differed from that in the normal 2SA cells, with a less compact structure. Therefore, after electrophoresis, the gel was subjected to SDS treatment to dissolve the complex structures, followed by membrane transfer. The results revealed ND1 in the 2SA and 2KD cells after SDS treatment (Figure 4B, right panel), suggesting that 2KD cells form an unstable complex with a different structure than normal.

Next, complex II was confirmed to be formed in all cells (Figure 4C). Complex III_2 was also formed in all cells, but complex III_2 + IV was formed less frequently in the 2SD cells (Figure 4D). Supercomplex was formed in the 2SA and 2KD cells, and the simple substance UQCRC1, a subunit of complex III_2, was detected only in the 2SD cells (Figure 4D). There was a lower rate of complex IV formation in the 2SD cells, and complex III_2 + IV and supercomplex were observed only in the 2SA and 2KD cells (Figure 4E). Immunoblotting of complex V subunits ATP5A1 and ATP6 showed less complex V formation in the 2SD cells

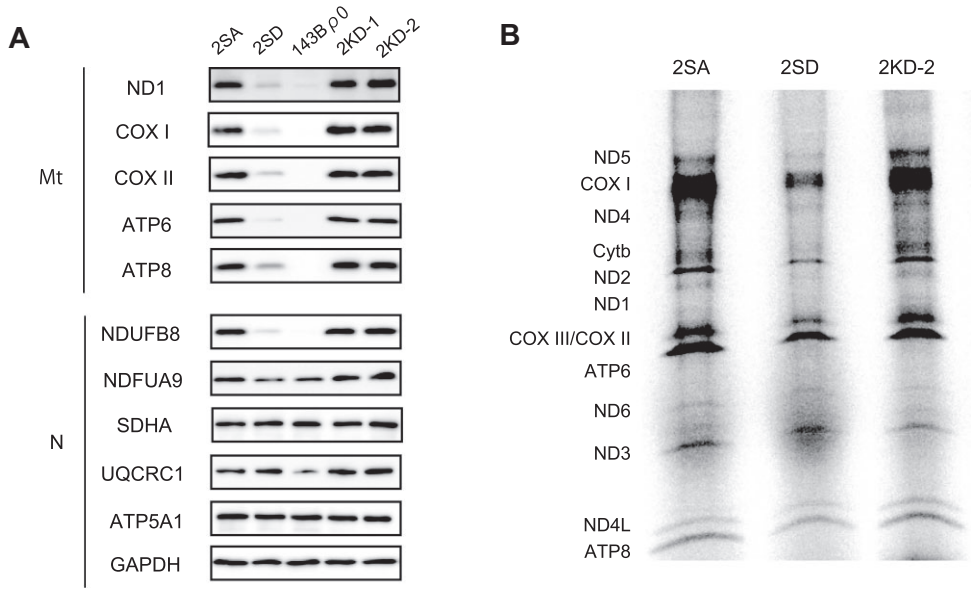

Figure 3. Improvements in protein expression and polypeptide synthesis. (**A**) Expression of mitochondrial proteins. Five micrograms of protein for each sample were loaded and blots were incubated with the indicated antibodies. Lane 1, 2SA cells; lane 2, 2SD cells; lane 3, 143Bρ0 cells; lane 4, 2KD-1 cells; lane 5, 2KD-2 cells. Mt: OXPHOS protein encoded by mtDNA; N: OXPHOS protein encoded by nuclear DNA. (**B**) 2SA, 2SD and 2KD-2 cells were pulse-labeled during the reaction with a mixture of [^{35}S]-methionine and [^{35}S]-cysteine in the presence of emetine, and then detected by autoradiography after SDS-PAGE. Each protein encoded by mtDNA is indicated on the left.

than in the 2SA and 2KD cells (Figure 4F). There was also a higher rate of complex V dimer formation in the 2SA cells for ATP6 (F_o domain), and incompletely formed subcomplexes were detected in the 2SD and 2KD cells for ATP5A1 (F_1 domain) (Figure 4F). This indicates that the 2KD cells partially formed incomplete complexes, even for complex V. These results suggested that oxidative phosphorylation in the 2KD cells may not have been completely improved due to the incompleteness of the respiratory chain complex, despite all of the complexes being present at the same level as in the 2SA cells.

τm^{5}u modification rate is partially restored in 2KD cells

Reduced mt tRNA$^{Leu(UUR)}$ stability and defective τm^{5}U modifications have been reported in MELAS patients with the 3243A > G mutation (6,16). Therefore, we performed northern blotting to analyze steady-state level of mt tRNA$^{Leu(UUR)}$. Owing to the presence of two mutations (3243A > G and 3290T > C) in mt tRNA$^{Leu(UUR)}$, a common DNA probe was not available. Therefore, we used two different probes to compare 2SA to 2SD, and 2SD to 2KD, respectively. The radio-labeled band of mt tRNA$^{Leu(UUR)}$ in each cell was normalized by 5S rRNA. Steady-state level of mt tRNA$^{Leu(UUR)}$ was significantly reduced in the 2SD cells (38%) relative to that in the 2SA cells (100%) (Figure 5A, left panels), whereas it was slightly but significantly increased in 2KD-2 cells (55%) (Figure 5A, right panels). Next, we measured τm^{5}U frequency of mt tRNA$^{Leu(UUR)}$ by a primer extension method assisted by chemical derivatization of τm^{5}U with CMC (31). We confirmed notable reduction of τm^{5}U frequency in 2SD cells (32%) compared to that in 2SA cells (100%) and found a significant increase of τm^{5}U frequency in 2KD-2 cells (59%) (Figure 5B). These findings suggest that 3290T > C haplotypic mutation contributes to partial recovery of steady-state level and τm^{5}U frequency of mt tRNA$^{Leu(UUR)}$ with 3243A > G mutation, thereby improving mitochondrial translation and respiratory activity.

Mt tRNA$^{Leu(UUR)}$ with the 3243A > G mutation and 3290T > C SNP has a different structure than mt tRNA$^{Leu(UUR)}$ with the 3243A > G mutation

The abnormal tRNA conformation and decreased aminoacylation have been reported in mt tRNA$^{Leu(UUR)}$ with the 3243A > G mutation (6,22). Therefore, we conducted melt curve analysis based on the intercalation of the SYBR Green I fluorophore to confirm the structural differences of mt tRNA$^{Leu(UUR)}$ in wild-type, 3243A > G mutation, and 3243A > G mutation with 3290T > C SNP. When double-stranded nucleic acid bound to SYBR Green I fluorophore is thermally denatured, the fluorophore is released and the fluorescence signal rapidly decreases at the melting temperature (T_m). Then, plotting this negative derivative (Δ fluorescence / Δ temperature) against the temperature, we get the melting curve of each nucleic acid. For that reason, any changes of tertiary structure and stability in mt tRNA$^{Leu(UUR)}$ can alter the melting curves profiles (34). The T_m values of mt tRNA$^{Leu(UUR)}$ were 68.8 ± 0.4°C in wild-type, 62.3 ± 0.9°C in 3243A > G mutation, and 64.4 ± 0.9°C in 3243A > G mutation with 3290T > C SNP (Figure 5C). We also confirmed that these unfolding curves are different from those of RNase A-treated wild-type mt tRNA$^{Leu(UUR)}$ and No RNA samples (Supplementary Figure S5). In addition, to confirm that these melting curves were derived from mt tRNA$^{Leu(UUR)}$, we performed

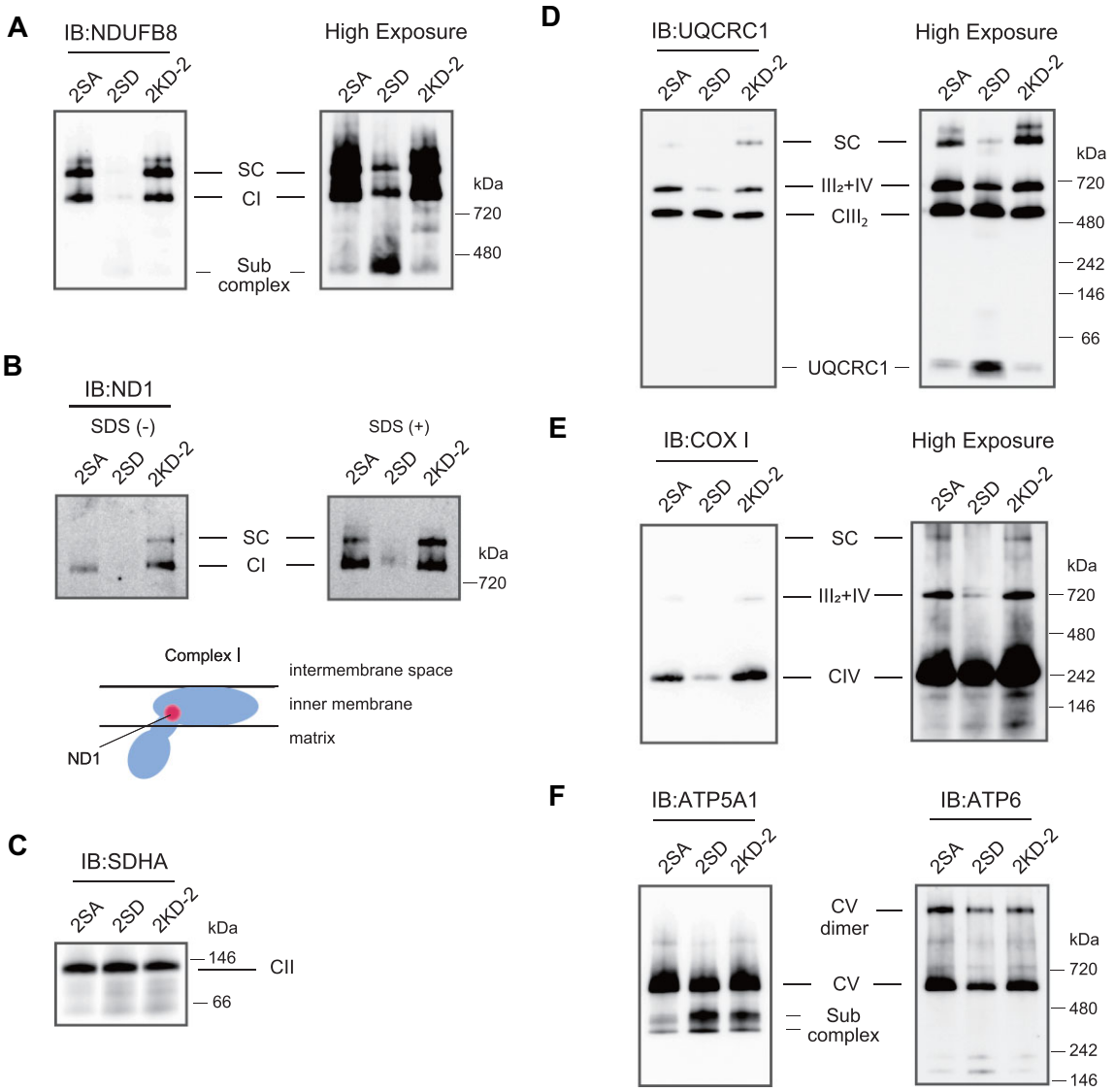

Figure 4. Partially incomplete respiratory chain complexes in the 2KD cells. The formation of respiratory chain complexes was assessed by BN-PAGE analysis. (**A**) Immunoblotting with NDUFB8 antibody. C I, complex I; SC, supercomplex formed by complexes I, III_2 and IV. (**B**) Immunoblotting with ND1 antibody. Before transferring proteins to membrane, the polyacrylamide gel was put in SDS buffer to loosen the complexes (right panel). (**C**) Immunoblotting with SDHA antibody. C II, complex II. (**D**) Immunoblotting with UQCRC1 antibody. $CIII_2$, dimeric complex III; III_2 + IV, supercomplex formed by complexes III_2 and IV; SC, supercomplex formed by complexes I, III_2, and IV. (**E**) Immunoblotting with COX I antibody. C IV, complex IV. (**F**) Immunoblotting with ATP5A1 (left panel) and ATP6 (right panel) antibody. CV, complex V; CV dimer, dimer formation of complex V; Subcomplex, complex containing F_1 subunits. The molecular masses (in kDa) of the molecular mass standards are shown.

electrophoresis using the samples after the *in vitro* transcription. We showed that only pure mt $tRNA^{Leu(UUR)}$ generated by *in vitro* transcription was present (Figure 5D).

Next, we analyzed aminoacylation status of mt $tRNA^{Leu(UUR)}$ by acid-urea northern blotting. We confirmed a significant reduction of the aminoacylation level in 2SD cells (78%) compared to that in 2SA cells (100%) (Supplementary Figure S6). In contrast, the aminoacylation level in 2KD-2 cells (91%) tended to improve compared to that in 2SD cells, but not significantly (Supplementary Figure S6). However, the lack of improvement in aminoacylation suggests that the mutation did not directly lead to an improvement in oxidative phosphorylation capacity.

Metabolite characteristics of patients with 3243A > G mutation with 3290T > C SNP

To evaluate the effects of mitochondrial dysfunction on metabolism, metabolomic analysis was performed using plasma from patients with mitochondrial disease. Three groups of patients were analyzed: patients with the 3243A > G mutation with 3290T > C SNP, MIDD patients with the 3243A > G mutation, and controls (Supplementary Table S3). Biochemical tests, including lactate and hematological tests on blood samples from healthy subjects, gave normal results. However, when we examined the differences among the groups, principal component analysis (PCA), a first-pass method to identify chemical

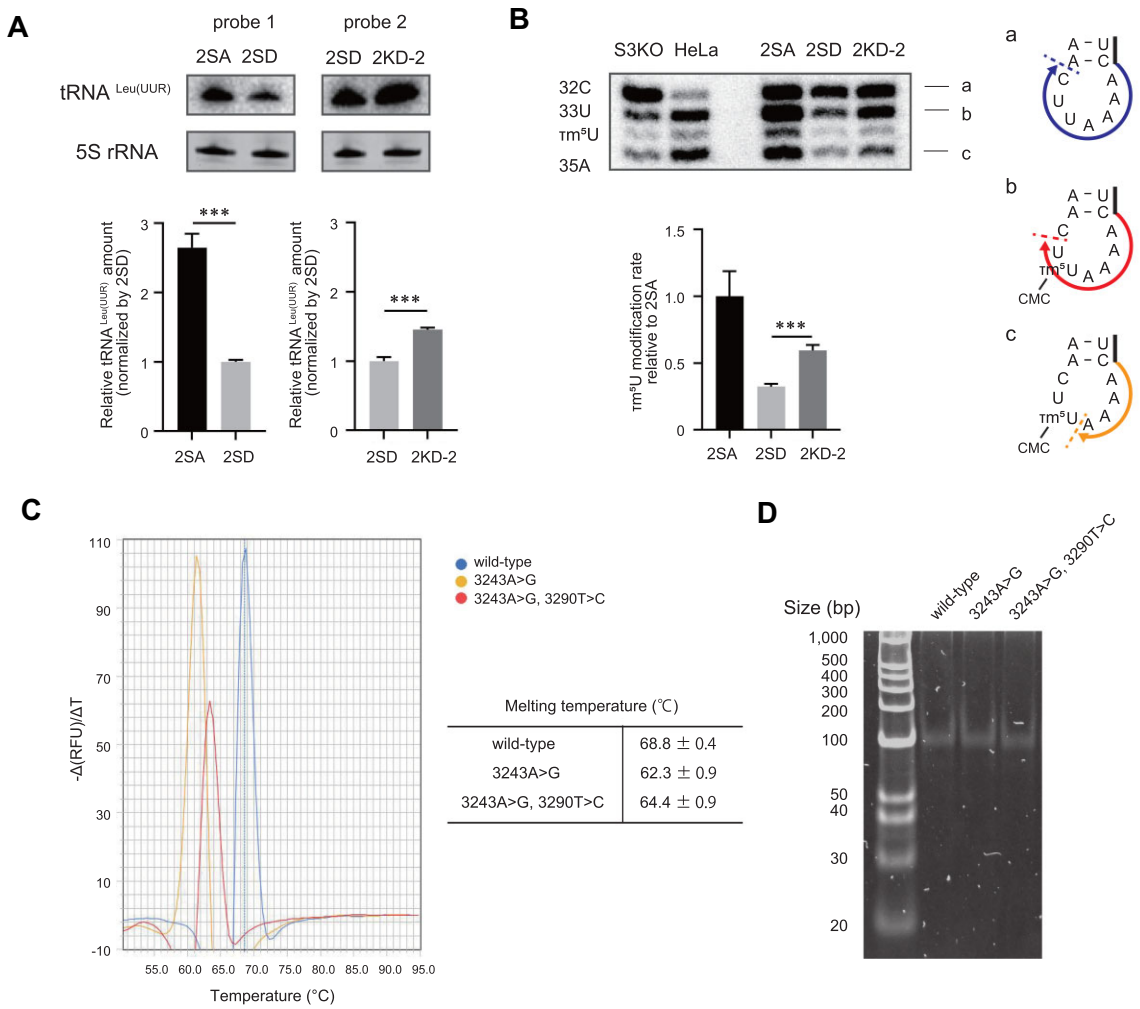

Figure 5. Improvements in the steady-state level and τm^5U modification rate of mt $tRNA^{Leu(UUR)}$ in the 2KD cells. (**A**) Steady-state level of mt-$tRNA^{Leu(UUR)}$ in each cell line measured by northern blotting. Specific probe 1 and probe 2 were used to detect mt-$tRNA^{Leu(UUR)}$ in 2SA and 2SD (left panels) and 2SD and 2KD-2 (right panels), respectively. 5S rRNAs stained with EtBr are used as loading controls. The lower panel shows relative mt-$tRNA^{Leu(UUR)}$ levels normalized by that in 2SD. Results are expressed as the mean ± SD of three independent experiments. Statistical significance was assessed by Student's *t*-test, $^{***}P < 0.001$. (**B**) Measuring τm^5U frequency of mt-$tRNA^{Leu(UUR)}$ by CMC-PE for the 2SA, 2SD and 2KD-2 cells. CMC-PE was performed in the indicated cell lines (upper panel). cDNA stops at position 32 by inserting dideoxyguanosine (indicated in band a and blue arrow), at positions 33 (band b and red arrow) and 35 (band c and yellow arrow) by CMC-τm^5U34 are indicated on the right side. The intensity ratio of τm^5U was calculated as (b + c) / (a + b + c), and a calibration curve was prepared using HeLa and G3KO cells, which have known τm^5U modification rates of 96.3% and 0%, respectively. The τm^5U modification rate of each cell was calculated by applying the intensity ratio of τm^5U to the calibration curve (lower panel). Results are expressed as the mean ± SD of three independent experiments. Statistical significance was assessed by Student's t-test, $^{***}P < 0.001$. (**C**) The melt curve analysis of mt $tRNA^{Leu(UUR)}$ in wild-type, 3243A > G mutation, and 3243A > G mutation with 3290T > C. The unfolding curves are shown wild-type in blue, 3243A > G mutation in orange, and 3243A > G mutation with 3290T > C in red (left panel). Each melting temperature (T_m) is expressed the mean ± SD of three independent experiments (right panel). (**D**) The electrophoresis of mt $tRNA^{Leu(UUR)}$ in wild-type, 3243A > G mutation, and 3243A > G mutation with 3290T > C. Each mt $tRNA^{Leu(UUR)}$ used in the melt curve analysis consists of a single species.

differences between high-dimensional spectral measurements (44), failed to separate the three groups due to strong overlap among them. Nonetheless, partial least squares discriminant analysis (PLS-DA) managed to separate the three groups, indicating that each group had a different metabolic profile (Figure 6A). Metabolites, including lactate, arginine, and citrulline, had the highest VIP (variable importance in the projection) scores, a prediction of the importance in the PLS model (45). Therefore, these metabolites were shown to have influenced the separation of each group (Figure 6B). In addition, the classical markers of lactate, pyruvate, and alanine tended to be elevated in the disease group relative to their levels in the control group, with a particularly large increase being observed for lactate in the 3243A > G with 3290T > C group (Figure 6C). In the 3243A > G with 3290T > C group, arginine and citrulline were significantly decreased compared with those in the control group, while citrulline was also significantly lower than that in the 3243A > G MIDD group (Figure 6C). In the 3243A > G MIDD group, methionine, dimethylglycine, aminobutyric acid, and epinephrine were significantly different from the levels in the control group and the 3243A > G with 3290T > C group (Figure 6C). Reduced glutathione was significantly reduced compared with that

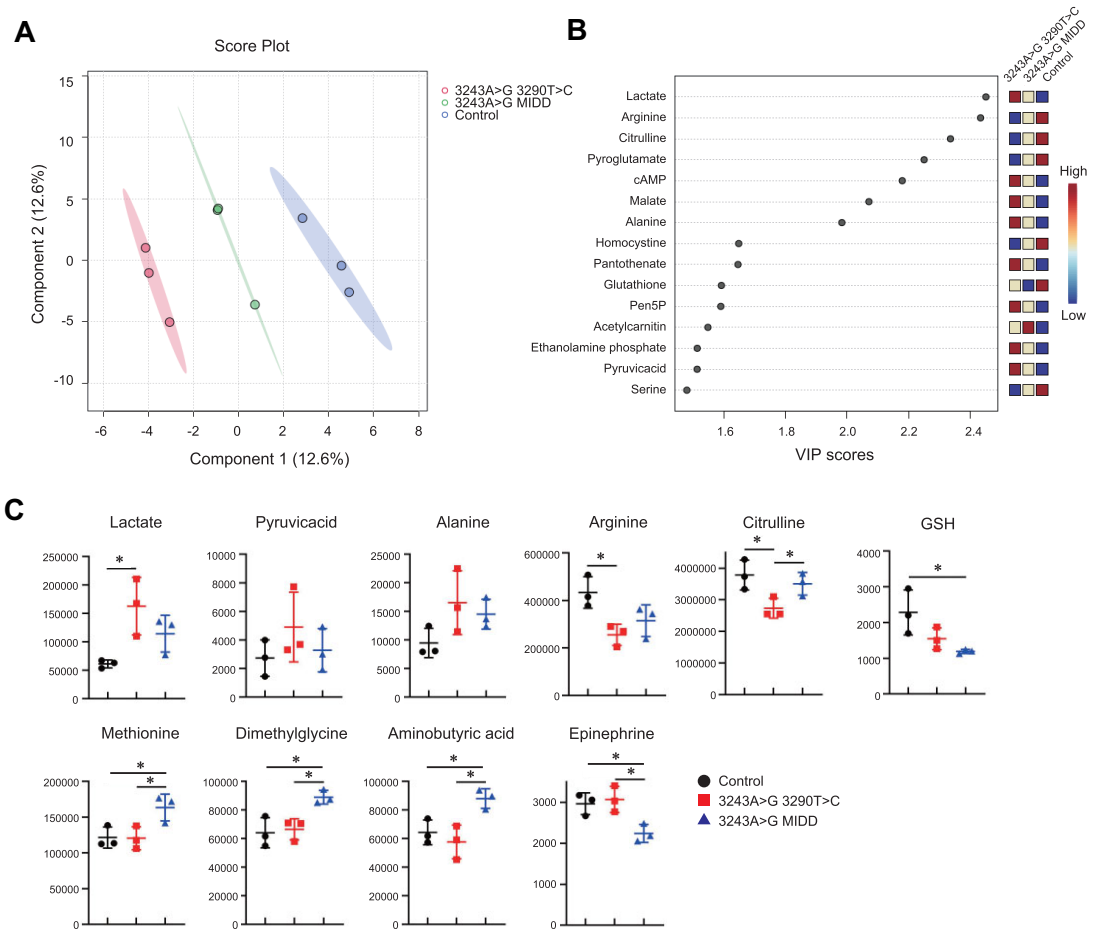

Figure 6. LC-MS metabolomic analysis in the 3243A > G with 3290T > C, 3243A > G MIDD and control groups. (**A**) Partial least squares discriminant analysis (PLS-DA) discriminating three groups. Red point, 3243A > G with 3290T > C group; green point, 3243A > G MIDD group; blue point, control group. (**B**) VIP score represents the importance for distinguishing three groups by PLS-DA. The colored boxes on the right show the relative concentration of the corresponding metabolite in each group. (**C**) Characteristic metabolites in 3243A > G with 3290T > C group ($n = 3$) and 3243A > G MIDD group ($n = 3$). Results are expressed as the mean ± SD of three independent experiments. Statistical significance was assessed by Student's *t*-test, $^*P < 0.05$.

in the control group (Figure 6C). These results suggest that lactate, arginine, and citrulline are characteristic metabolites of the 3243A > G with 3290T > C group and may serve as markers to distinguish patients with the 3243A > G mutation and controls. In addition, methionine, dimethylglycine, aminobutyric acid, epinephrine, and reduced glutathione are characteristic metabolites of the 3243A > G MIDD group and not of the 3243A > G with 3290T > C group.

DISCUSSION

In this study, we found that the presence of both the 3243A > G mutation and the 3290T > C SNP in mt $tRNA^{Leu(UUR)}$ gene partially improved the rate of τm^5U modification, restoring mitochondrial translation function, respiratory chain complex formation, and mitochondrial function compared to MELAS cells with only the 3243A > G mutation. The 3290T > C is an SNP possessed by haplogroup F4a and is widely found in Southeast Asia, such as Taiwan, China, and Japan. The overall frequency of the 3290T > C SNP in mt $tRNA^{Leu(UUR)}$ gene is about 0.22%, and this haplotypic mutation is supposed to implicate in the pathogenesis of the disease in the Chinese Han hypertensives (46). However, no association with hypertension was found for the four individuals in this study.

Liu et al. reported that a high rate of 3243A > G heteroplasmy was observed in peripheral blood not only in a proband diagnosed with mitochondrial myopathy and showing dyspnea but also in asymptomatic family members in Han Chinese families belonging to haplogroup F4a (26). In addition, some case reports have indicated that the presence of the 3290T > C SNP affects the clinical phenotype (25,26), while a few reports have confirmed patients with the 3243A > G mutation showing respiratory failure as an early clinical feature in Asian countries (47–51). Although haplogroup analysis has not been conducted in these patients, we considered that they are likely to have the 3290T > C SNP in common. Kamakura et al. assumed that the increase of abnormal mitochondria in the diaphragm may lead to weakness of respiratory muscle and respiratory failure (47), but detailed analysis and determination of the mechanism involved have not been performed.

A heteroplasmic mutation, G12300A, in another mt leucine tRNA gene, mt $tRNA^{Leu(CUN)}$, which functions as a suppressor of respiratory failure, including the 3243A > G mutation, has been reported (52). To suppress the MELAS mutation, it is important to acquire a wobble modification in the other $tRNA^{Leu(CUN)}$ (53). The finding of a 3290T > C haplotypic mutation in mt $tRNA^{Leu(UUR)}$ that restores taurine modification by conformational change suggests a new molecular mechanism for MELAS.

The clinical presentation caused by the 3243A > G mutation depends on the organs or tissues in which the mutated mtDNA is distributed. In non-meristematic tissue such as skeletal muscle, the rate of 3243A > G heteroplasmy correlates with age and disease severity. Meanwhile, in peripheral blood, the rate of 3243A > G heteroplasmy decreases exponentially with age because hematopoietic stem cells with high 3243A > G heteroplasmy are selectively eliminated (22,23). However, patients with the 3243A > G mutation with the 3290T > C SNP retained a 3243A > G heteroplasmy rate of more than 90% in peripheral blood (Figure 1D). This indicates that cells with the 3243A > G mutation with 3290T > C SNP have not been eliminated; in other words, mitochondrial function have not been reduced to the extent that it exceeded the threshold of selective exclusion.

The 3243A > G cybrid cells (2SD cells) have been reported to exhibit decreases in mitochondrial protein synthesis, respiratory chain enzyme activity, and oxygen consumption (6,12–14). This study also confirmed that mitochondrial function was greatly reduced in the 2SD cells. Meanwhile, mitochondrial function was improved in the 2KD cells with the 3243A > G mutation and 3290T > C SNP. In particular, the subunits of the mitochondrial respiratory chain encoded by mtDNA were expressed to the same extent as in wild-type 2SA cells (Figure 3A). However, the levels of subunit expression do not necessarily correlate with respiratory chain enzyme activity or functional complex formation (6,15). In fact, the oxygen consumption of the 2KD cells was only around half that of the 2SA cells (Figure 2C). This was probably due to the presence of some unstable and incomplete respiratory chain complexes in the 2KD cells because complete recovery of the τm^5U modification in mt $tRNA^{Leu(UUR)}$ had not occurred and translational rate was incomplete.

Activity of the mitochondrial respiratory chain, including complex I, has been reported to be decreased in MELAS patients (8). In this study, MELAS 3243A > G cells (2SD cells) showed markedly decreased expression not only of ND1 encoded by mtDNA but also of NDUFB8 and NDUFA9 encoded in the nucleus (Figure 3A); this indicates destabilization of complex I. Meanwhile, the steady-state levels of ND1, NDUFB8 and NDUFA9 were improved in the 2KD cells (Figure 3A). These results are also consistent with the results of complex I formation (Figure 4A). However, oxygen consumption was reduced by around half in the 2KD cells compared with that in the 2SA cells. Thus, even in the 2KD cells, which show improvement in τm^5U modification, there may be structural and functional defects in complex I, which is particularly affected by τm^5U modification. Complexes III and IV contain one and three subunits encoded by mtDNA, respectively, and they have a low proportion of UUG codons. Thus, these complexes are expected not to show as much destabilization or loss of function as complex I (Figure 4).

Complex V is composed of two domains: membrane-extrinsic and matrix-facing F_1 plus membrane-intrinsic F_o. The formation of the F_1 domain is followed by the assembly of various subunits, and finally mtDNA-encoded ATP6 and ATP8 are incorporated into the F_o domain. However, the inhibition of mitochondrial translation results in the accumulation of complex V intermediates (subcomplexes) prior to ATP6 and ATP8 insertion, and the steady-state level of complex V is also reduced (54–56). In this study, we detected subcomplexes in the 2SD and 2KD cells when the formation of complex V was confirmed for ATP5A1, a subunit in F_1 domain (Figure 4F). Subcomplex formation was particularly pronounced in the 2SD cells, but was rarely detected in the wild-type 2SA cells. This suggests that the amount of subcomplex increases with increasing impairment of the mitochondrial translational function, leading to decreased activity of complex V.

Complex V dimers are also important for mitochondrial morphology because they are involved in the formation of the lamellar and highly curved crista ridges (57–60). In the 2KD cells, slight abnormalities were considered to be in mitochondrial morphology because there was less formation of complex V dimers (Figure 2D & 4F). In fact, the 2SA cells had more filamentous mitochondria, while the 2SD cells had more fragmented ones, indicating mitochondrial dysfunction (Figure 2D). The decrease of dimers as well as monomers is considered to be one reason for the decline in mitochondrial function, including oxidative phosphorylation.

Next, we focused on the synthesis rate and defects of the mtDNA-encoded proteins with respect to complex destabilization. In the 2SD cells, few of the seven subunits of complex I were synthesized except for ND2 and ND3; this would result in the much low rate of formation of complex I (Figures 3B & 4A). Meanwhile, the rate of formation of complex IV was decreased, even though the synthesis of complex IV subunits COX I, II, and III was confirmed (Figures 3B and 4E). Therefore, the synthesized subunits are likely to be fragile before they form a complex or the formed complexes are fragile. Indeed, it has been reported that reduced subunit synthesis itself is not a factor leading to decreased respiratory activity or oxygen consumption (16,61). In the 2KD cells, the steady-state level of each subunit was completely improved and complex formation was comparable to that in the 2SA cells, although the overall synthesis rate was lower than that in the 2SA cells (Figures 3A, B and 4). Therefore, the mechanisms of synthesis and degradation of mitochondrial proteins in the 2KD cells may differ from normal 2SA cells.

The formation of τm^5U in mt tRNA anticodon is catalyzed by an enzyme complex, MTO1 and GTPBP3. When mt $tRNA^{Leu(UUR)}$ has one of five different point mutations (3243A > G, 3244G > A, 3258T > C, 3271T > C and 3291T > C) derived from patients showing the clinical features of MELAS, a lack of τm^5U modification has been confirmed (16). In a model structure of the MTO1 complexed with tRNA, four mutations (with the exception of 3271T > C) were shown to be located at the interface contacting the modifying enzyme (22). Therefore, it is assumed

that these mutations may impair recognition of the mutant mt tRNA$^{Leu(UUR)}$s by MTO1 (18–22).

In the L-shaped tertiary structure of mt tRNA$^{Leu(UUR)}$, long-range interactions take place between residues U8-A14-A21, R15-Y48, G18-Y55 and G19-C56 (62,63). However, the 3243A > G (A14 in tRNA numbering) can disrupt the tertiary interaction of U8-A14-A21, and makes mt tRNA$^{Leu(UUR)}$ structure fragile (22). We thought that 3290T > C SNP, corresponding to U > C at position 59 in mt tRNA$^{Leu(UUR)}$, enhances a proper conformation of mt tRNA$^{Leu(UUR)}$ with the 3243A > G mutation and improves binding affinity to MTO1 by taking place a new tertiary interaction in C59. As for the levels of mt tRNA$^{Leu(UUR)}$, those of cybrid cells with the 3243A > G mutation derived from a MELAS patient have been reported to be reduced to approximately 30–50% of the levels in wild-type cells, which has been considered to be due to mt tRNA$^{Leu(UUR)}$ with the 3243A > G mutation being easily degraded (7,9). On the other hand, mt tRNA$^{Leu(UUR)}$ levels in the 2KD cells were significantly improved relative to those in the 2SD cells in this study (Figure 5A). This also suggests that the 3290T > C SNP is likely to stabilize the structure of mt tRNA$^{Leu(UUR)}$ with the 3243A > G mutation. Actually, we have shown that mt tRNA$^{Leu(UUR)}$ with the 3290T > C SNP in addition to 3243A > G mutation has a different structure compared to that with the only 3243A > G mutation in melting curve analysis (Figure 5C). However, it should be considered that this structural analysis was obtained using mt tRNA$^{Leu(UUR)}$ without post-transcriptional modifications.

We also confirmed that lactate levels in plasma were significantly higher in patients with the 3243A > G mutation and 3290T > C SNP (Figure 1D). Classical markers, such as lactate, pyruvate, and alanine, are elevated in mitochondrial diseases (5,64,65), but we thought that the significantly high levels of lactate may be associated with the respiratory symptoms of patients with the 3243A > G mutation and 3290T > C SNP (Figure 6C). Lena et al. reported that arginine levels in plasma are decreased in sleep apnea (66), and thus we assumed that the low levels of arginine in patients with the 3243A > G mutation and 3290T > C SNP may also be associated with respiratory symptoms (Figure 6C). Glutathione, which was significantly decreased only in MIDD patients when compared with the level in controls (Figure 6C), is an antioxidant that protects cells from reactive oxygen species. Therefore, patients with the 3243A > G mutation and 3290T > C SNP may also have resistance to oxidative stress similar to controls. In addition, *GDF15* is known as a biomarker whose expression increases with increasing clinical severity of mitochondrial disease, and its levels in blood samples and cybrid cells derived from MELAS patients have been shown to be elevated in metabolomic analysis (5,67–69). In this study, the expression of *GDF15* was reduced in the 2KD cells compared with that in the 2SD cells (Figure 2B), which is likely to reflect a restoration of mitochondrial function. From these analyses, we confirmed that patients with the 3243A > G mutation have different metabolic profiles depending on the clinical presentation. This shows the potential to establish biomarkers for various diseases with 3243A > G mutation other than MELAS.

In this study, we showed that 3290T > C haplotypic mutation improved mitochondrial function and clinical symptoms of patients with 3243A > G mutation. This work would contribute to our understanding of the mechanism that improves τm^5U modification and aid the development of new therapeutic agents for MELAS by discovering small molecules that have the effect of bringing mt tRNA$^{Leu(UUR)}$ structure closer to normal.

DATA AVAILABILITY

All data generated or analyzed during this study are included in this article (and its Supplementary Information files).

SUPPLEMENTARY DATA

Supplementary Data are available at NAR Online.

ACKNOWLEDGEMENTS

We would like to thank Edanz for English language editing.

FUNDING

Japan Society for the Promotion of Science [(20H00530, 21K11678, 22H03537, 21H04278) to K.D. and T.U.]; ERATO (JPMJER2002) from JST (to T.S.). Funding for open access charge: Japan Society for the Promotion of Science.
Conflict of interest statement. None declared.

This paper is linked to: doi:10.1093/nar/gkad139.

REFERENCES

1. Goto,Y.-i., Nonaka,I. and Horai,S. (1990) A mutation in the tRNALeu (UUR) gene associated with the MELAS subgroup of mitochondrial encephalomyopathies. *Nature*, **348**, 651–653.
2. Suzuki,Y., Nishimaki,K., Taniyama,M., Muramatsu,T., Atsumi,Y., Matsuoka,K. and Ohta,S. (2004) Lipoma and opthalmoplegia in mitochondrial diabetes associated with small heteroplasmy level of 3243 tRNALeu (UUR) mutation. *Diabetes Res. Clin. Pract.*, **63**, 225–229.
3. Momiyama,Y., Atsumi,Y., Ohsuzu,F., Ui,S., Morinaga,S., Matsuoka,K. and Kimura,M. (1999) Rapid progression of cardiomyopathy in mitochondrial diabetes. *Jpn. Circ. J.*, **63**, 130–132.
4. Yatsuga,S., Povalko,N., Nishioka,J., Katayama,K., Kakimoto,N., Matsuishi,T., Kakuma,T., Koga,Y. and Grp,T.M.M.S. (2012) MELAS: a nationwide prospective cohort study of 96 patients in Japan. *Biochim. Biophys. Acta, Gen. Subj.*, **1820**, 619–624.
5. Sharma,R., Reinstadler,B., Engelstad,K., Skinner,O.S., Stackowitz,E., Haller,R.G., Clish,C.B., Pierce,K., Walker,M.A., Fryer,R. *et al.* (2021) Circulating markers of NADH-reductive stress correlate with mitochondrial disease severity. *J. Clin. Invest.*, **131**, e136055.
6. Kirino,Y., Yasukawa,T., Ohta,S., Akira,S., Ishihara,K., Watanabe,K. and Suzuki,T. (2004) Codon-specific translational defect caused by a wobble modification deficiency in mutant tRNA from a human mitochondrial disease. *Proc. Natl. Acad. Sci. U.S.A.*, **101**, 15070–15075.
7. Yasukawa,T., Suzuki,T., Suzuki,T., Ueda,T., Ohta,S. and Watanabe,K. (2000) Modification defect at anticodon wobble nucleotide of mitochondrial tRNAsLeu (UUR) with pathogenic mutations of mitochondrial myopathy, encephalopathy, lactic acidosis, and stroke-like episodes. *J. Biol. Chem.*, **275**, 4251–4257.

8. Koga,Y., Nonaka,I., Kobayashi,M., Tojyo,M. and Nihei,K. (1988) Muscle pathology in complex I (NADH CoQ reductase) deficiency. *Ann. Neurol.*, **24**, 749–756.
9. Chomyn,A., Enriquez,J.A., Micol,V., Fernandez-Silva,P. and Attardi,G. (2000) The mitochondrial myopathy, encephalopathy, lactic acidosis, and stroke-like episode syndrome-associated human mitochondrial tRNALeu (UUR) mutation causes aminoacylation deficiency and concomitant reduced association of mRNA with ribosomes. *J. Biol. Chem.*, **275**, 19198–19209.
10. Hess,J.F., Parisi,M.A., Bennett,J.L. and Clayton,D.A. (1991) Impairment of mitochondrial transcription termination by a point mutation associated with the MELAS subgroup of mitochondrial encephalomyopathies. *Nature*, **351**, 236–239.
11. Flierl,A., Reichmann,H. and Seibel,P. (1997) Pathophysiology of the MELAS 3243 transition mutation. *J. Biol. Chem.*, **272**, 27189–27196.
12. Dunbar,D., Moonie,P., Zeviani,M. and Holt,I. (1996) Complex I deficiency is associated with 3243G: c mitochondrial DNA in osteosarcoma cell cybrids. *Hum. Mol. Genet.*, **5**, 123–129.
13. Chomyn,A., Martinuzzi,A., Yoneda,M., Daga,A., Hurko,O., Johns,D., Lai,S., Nonaka,I., Angelini,C. and Attardi,G. (1992) MELAS mutation in mtDNA binding site for transcription termination factor causes defects in protein synthesis and in respiration but no change in levels of upstream and downstream mature transcripts. *Proc. Natl. Acad. Sci. U.S.A.*, **89**, 4221–4225.
14. Hayashi,J.-I., Ohta,S., Takai,D., Miyabayashi,S., Sakuta,R., Goto,Y. and Nonaka,I. (1993) Accumulation of mtDNA with a mutation at position 3271 in tRNALeu (UUR) gene introduced from a MELAS patient to HeLa cells lacking mtDNA results in progressive inhibition of mitochondrial respiratory function. *Biochem. Biophys. Res. Commun.*, **197**, 1049–1055.
15. Sasarman,F., Antonicka,H. and Shoubridge,E.A. (2008) The A3243G tRNALeu (UUR) MELAS mutation causes amino acid misincorporation and a combined respiratory chain assembly defect partially suppressed by overexpression of EFTu and EFG2. *Hum. Mol. Genet.*, **17**, 3697–3707.
16. Kirino,Y., Goto,Y.-i., Campos,Y., Arenas,J. and Suzuki,T. (2005) Specific correlation between the wobble modification deficiency in mutant tRNAs and the clinical features of a human mitochondrial disease. *Proc. Natl. Acad. Sci. U.S.A.*, **102**, 7127–7132.
17. Asano,K., Suzuki,T., Saito,A., Wei,F.Y., Ikeuchi,Y., Numata,T., Tanaka,R., Yamane,Y., Yamamoto,T., Goto,T. *et al.* (2018) Metabolic and chemical regulation of tRNA modification associated with taurine deficiency and human disease. *Nucleic. Acids. Res.*, **46**, 1565–1583.
18. Li,X. and Guan,M.-X. (2002) A human mitochondrial GTP binding protein related to tRNA modification may modulate phenotypic expression of the deafness-associated mitochondrial 12S rRNA mutation. *Mol. Cell. Biol.*, **22**, 7701–7711.
19. Osawa,T., Ito,K., Inanaga,H., Nureki,O., Tomita,K. and Numata,T. (2009) Conserved cysteine residues of GidA are essential for biogenesis of 5-carboxymethylaminomethyluridine at tRNA anticodon. *Structure*, **17**, 713–724.
20. Meyer,S., Scrima,A., Versées,W. and Wittinghofer,A. (2008) Crystal structures of the conserved tRNA-modifying enzyme GidA: implications for its interaction with MnmE and substrate. *J. Mol. Biol.*, **380**, 532–547.
21. Umeda,N., Suzuki,T., Yukawa,M., Ohya,Y., Shindo,H., Watanabe,K. and Suzuki,T. (2005) Mitochondria-specific RNA-modifying enzymes responsible for the biosynthesis of the wobble base in mitochondrial tRNAs: implications for the molecular pathogenesis of human mitochondrial diseases. *J. Biol. Chem.*, **280**, 1613–1624.
22. Suzuki,T., Nagao,A. and Suzuki,T. (2011) Human mitochondrial tRNAs: biogenesis, function, structural aspects, and diseases. *Annu. Rev. Genet.*, **45**, 299–329.
23. Rajasimha,H.K., Chinnery,P.F. and Samuels,D.C. (2008) Selection against pathogenic mtDNA mutations in a stem cell population leads to the loss of the 3243A→ G mutation in blood. *Am. J. Hum. Genet.*, **82**, 333–343.
24. Chinnery,P.F., Howell,N., Lightowlers,R.N. and Turnbull,D.M. (1997) Molecular pathology of MELAS and MERRF. The relationship between mutation load and clinical phenotypes. *Brain*, **120**, 1713–1721.
25. Hammans,S., Sweeney,M., Hanna,M., Brockington,M., Morgan-Hughes,J. and Harding,A. (1995) The mitochondrial DNA transfer RNA leu (UUR) A→ G (3243) mutation: a clinical and genetic study. *Brain*, **118**, 721–734.
26. Liu,G., Shen,X., Sun,Y., Lv,Q., Li,Y. and Du,A. (2020) Heteroplasmy and phenotype spectrum of the mitochondrial tRNALeu (UUR) gene m. 3243A>G mutation in seven Han Chinese families. *J. Neurol. Sci.*, **408**, 116562.
27. Chomyn,A. (1996) In: *Methods Enzymol*. Elsevier, Vol. **264**, pp. 334–339.
28. Yagi,M., Uchiumi,T., Takazaki,S., Okuno,B., Nomura,M., Yoshida,S.-i., Kanki,T. and Kang,D. (2012) p32/gC1qR is indispensable for fetal development and mitochondrial translation: importance of its RNA-binding ability. *Nucleic Acids Res.*, **40**, 9717–9737.
29. Yagi,M., Toshima,T., Amamoto,R., Do,Y., Hirai,H., Setoyama,D., Kang,D. and Uchiumi,T. (2021) Mitochondrial translation deficiency impairs NAD+-mediated lysosomal acidification. *EMBO J.*, **40**, e105268.
30. Saito,T., Uchiumi,T., Yagi,M., Amamoto,R., Setoyama,D., Matsushima,Y. and Kang,D. (2017) Cardiomyocyte-specific loss of mitochondrial p32/C1qbp causes cardiomyopathy and activates stress responses. *Cardiovasc. Res.*, **113**, 1173–1185.
31. Tomoda,E., Nagao,A., Shirai,Y., Asano,K., Suzuki,T., Battersby,B.J. and Suzuki,T. (2023) Restoration of mitochondrial function through activation of hypomodified tRNAs with pathogenic mutations associated with mitochondrial diseases. *Nucleic Acids Res.*, https://doi.org/10.1093/nar/gkad139.
32. Suzuki,T., Yashiro,Y., Kikuchi,I., Ishigami,Y., Saito,H., Matsuzawa,I., Okada,S., Mito,M., Iwasaki,S., Ma,D. *et al.* (2020) Complete chemical structures of human mitochondrial tRNAs. *Nat. Commun.*, **11**, 4269.
33. Lin,H., Miyauchi,K., Harada,T., Okita,R., Takeshita,E., Komaki,H., Fujioka,K., Yagasaki,H., Goto,Y., Yanaka,K. *et al.* (2018) CO2-sensitive tRNA modification associated with human mitochondrial disease. *Nat. Commun.*, **9**, 1875.
34. Holman,K.M., Puppala,A.K., Lee,J.W., Lee,H. and Simonović,M. (2017) Insights into substrate promiscuity of human seryl-tRNA synthetase. *RNA*, **23**, 1685–1699.
35. Varshney,U., Lee,C.-P. and RajBhandary,U.L. (1991) Direct analysis of aminoacylation levels of tRNAs in vivo. Application to studying recognition of Escherichia coli initiator tRNA mutants by glutaminyl-tRNA synthetase. *J. Biol. Chem.*, **266**, 24712–24718.
36. Nagao,A., Suzuki,T., Katoh,T., Sakaguchi,Y. and Suzuki,T. (2009) Biogenesis of glutaminyl-mt tRNAGln in human mitochondria. *Proc. Natl. Acad. Sci. U.S.A.*, **106**, 16209–16214.
37. Setoyama,D., Lee,H.Y., Moon,J.S., Tian,J., Kang,Y.E., Lee,J.H., Shong,M., Kang,D. and Yi,H.S. (2022) Immunometabolic signatures predict recovery from thyrotoxic myopathy in patients with Graves' disease. *J. Cachexia Sarcopenia Muscle*, **13**, 355–367.
38. Vance,J.E. (2014) MAM (mitochondria-associated membranes) in mammalian cells: lipids and beyond. *Biochim. Biophys. Acta*, **1841**, 595–609.
39. Veeresh,P., Kaur,H., Sarmah,D., Mounica,L., Verma,G., Kotian,V., Kesharwani,R., Kalia,K., Borah,A., Wang,X. *et al.* (2019) Endoplasmic reticulum-mitochondria crosstalk: from junction to function across neurological disorders. *Ann. N. Y. Acad. Sci.*, **1457**, 41–60.
40. Rambold,A.S., Kostelecky,B., Elia,N. and Lippincott-Schwartz,J. (2011) Tubular network formation protects mitochondria from autophagosomal degradation during nutrient starvation. *Proc. Natl. Acad. Sci. U.S.A.*, **108**, 10190–10195.
41. Kunz,T.C., Götz,R., Gao,S., Sauer,M. and Kozjak-Pavlovic,V. (2020) Using expansion microscopy to visualize and characterize the morphology of mitochondrial cristae. *Front. Cell Dev. Biol.*, **8**, 617.
42. Pascucci,B., Spadaro,F., Pietraforte,D., Nuccio,C.D., Visentin,S., Giglio,P., Dogliotti,E. and D'Errico,M. (2021) DRP1 Inhibition rescues mitochondrial integrity and excessive apoptosis in CS-A disease cell models. *Int. J. Mol. Sci.*, **22**, 7123.
43. Bakare,A.B., Daniel,J., Stabach,J., Rojas,A., Bell,A., Henry,B. and Iyer,S. (2021) Quantifying mitochondrial dynamics in patient fibroblasts with multiple developmental defects and mitochondrial disorders. *Int. J. Mol. Sci.*, **22**, 6263.
44. Worley,B. and Powers,R. (2016) PCA as a practical indicator of OPLS-DA model reliability. *Curr. Metabolomics*, **4**, 97–103.

45. Brunner,V., Hussein,M. and Becker,T. (2016) Biomass estimation in Pichia pastoris cultures by combined single-wavelength fluorescence measurements. *Biotechnol. Bioeng.*, **113**, 2394–2402.
46. Zhu,H.-Y., Wang,S.-W., Liu,L., Chen,R., Wang,L., Gong,X.-L. and Zhang,M.-L. (2009) Genetic variants in mitochondrial tRNA genes are associated with essential hypertension in a Chinese Han population. *Clin. Chim. Acta*, **410**, 64–69.
47. Kamakura,K., Abe,H., Tadano,Y., Nakamura,R., Kobayashi,H., Kawaguchi,S., Nagata,N., Matsuoka,T., Sakuta,R. and Nonaka,I. (1995) Recurrent respiratory failure in a patient with 3243 mutation in mitochondrial DNA. *J. Neurol.*, **242**, 253–255.
48. Pan,X., Wang,L., Fei,G., Dong,J., Zhong,C., Lu,J. and Jin,L. (2019) Acute respiratory failure is the initial manifestation in the adult-onset A3243G tRNALeu mtDNA mutation: a case report and the literature review. *Front. Neurol.*, **10**, 780.
49. Yang,C., Hwang,C., Pang,C. and Wei,Y. (1998) Mitochondrial myopathy with predominant respiratory dysfunction in a patient with A3243G mutation in the mitochondrial tRNA (Leu (UUR)) gene. *J. Formos. Med. Assoc.*, **97**, 715–719.
50. Chang,K., Mak,Y., Yu,W., Lau,K., Yan,W. and Chow,T. (2002) Respiratory insufficiency in a Chinese adult with mitochondrial myopathy. *Hong Kong Med. J.*, **8**, 137–140.
51. Amornvit,J., Pasutharnchat,N., Pachinburavan,M., Jongpiputvanich,S. and Joyjinda,Y. (2014) Fulminant respiratory muscle paralysis, an expanding clinical spectrum of mitochondrial A3243G tRNALeu mutation. *J. Med. Assoc. Thai.*, **97**, 467–472.
52. El Meziane,A., Lehtinen,S.K., Hance,N., Nijtmans,L.G., Dunbar,D., Holt,I.J. and Jacobs,H.T. (1998) A tRNA suppressor mutation in human mitochondria. *Nat. Genet.*, **18**, 350–353.
53. Kirino,Y., Yasukawa,T., Marjavaara,S.K., Jacobs,H.T., Holt,I.J., Watanabe,K. and Suzuki,T. (2006) Acquisition of the wobble modification in mitochondrial tRNALeu(CUN) bearing the G12300A mutation suppresses the MELAS molecular defect. *Hum. Mol. Genet.*, **15**, 897–904.
54. Signes,A. and Fernandez-Vizarra,E. (2018) Assembly of mammalian oxidative phosphorylation complexes I–V and supercomplexes. *Essays Biochem.*, **62**, 255–270.
55. Nijtmans,L.G., Klement,P., Houštěk,J. and van den Bogert,C. (1995) Assembly of mitochondrial ATP synthase in cultured human cells: implications for mitochondrial diseases. *Biochim. Biophys. Acta Mol. Basis Dis.*, **1272**, 190–198.
56. Wittig,I., Meyer,B., Heide,H., Steger,M., Bleier,L., Wumaier,Z., Karas,M. and Schägger,H. (2010) Assembly and oligomerization of human ATP synthase lacking mitochondrial subunits a and A6L. *Biochim. Biophys. Acta Bioenerg.*, **1797**, 1004–1011.
57. Dudkina,N.V., Heinemeyer,J., Keegstra,W., Boekema,E.J. and Braun,H.-P. (2005) Structure of dimeric ATP synthase from mitochondria: an angular association of monomers induces the strong curvature of the inner membrane. *FEBS Lett.*, **579**, 5769–5772.
58. Davies,K.M., Anselmi,C., Wittig,I., Faraldo-Gómez,J.D. and Kühlbrandt,W. (2012) Structure of the yeast F1Fo-ATP synthase dimer and its role in shaping the mitochondrial cristae. *Proc. Natl. Acad. Sci. U.S.A.*, **109**, 13602–13607.
59. He,J., Ford,H.C., Carroll,J., Ding,S., Fearnley,I.M. and Walker,J.E. (2017) Persistence of the mitochondrial permeability transition in the absence of subunit c of human ATP synthase. *Proc. Natl. Acad. Sci. U.S.A.*, **114**, 3409–3414.
60. Paumard,P., Vaillier,J., Coulary,B., Schaeffer,J., Soubannier,V., Mueller,D.M., Brèthes,D., di Rago,J.-P. and Velours,J. (2002) The ATP synthase is involved in generating mitochondrial cristae morphology. *EMBO J.*, **21**, 221–230.
61. Janssen,G.M., Maassen,J.A. and van den Ouweland,J.M. (1999) The diabetes-associated 3243 mutation in the mitochondrial tRNALeu (UUR) gene causes severe mitochondrial dysfunction without a strong decrease in protein synthesis rate. *J. Biol. Chem.*, **274**, 29744–29748.
62. HELM,M., BRULÉ,H., FRIEDE,D., GIEGÉ,R., Puetz,D. and FLORENTZ,C. (2000) Search for characteristic structural features of mammalian mitochondrial tRNAs. *RNA*, **6**, 1356–1379.
63. Sohm,B., Frugier,M., Brulé,H., Olszak,K., Przykorska,A. and Florentz,C. (2003) Towards understanding human mitochondrial leucine aminoacylation identity. *J. Mol. Biol.*, **328**, 995–1010.
64. Esterhuizen,K., Van der Westhuizen,F.H. and Louw,R. (2017) Metabolomics of mitochondrial disease. *Mitochondrion*, **35**, 97–110.
65. Rahman,J. and Rahman,S. (2018) Mitochondrial medicine in the omics era. *Lancet North Am. Ed.*, **391**, 2560–2574.
66. Lavie,L., Hefetz,A., Luboshitzky,R. and Lavie,P. (2003) Plasma levels of nitric oxide and L-arginine in sleep apnea patients. *J. Mol. Neurosci.*, **21**, 57–63.
67. Maresca,A., Del Dotto,V., Romagnoli,M., La Morgia,C., Di Vito,L., Capristo,M., Valentino,M.L. and Carelli,V. (2020) Expanding and validating the biomarkers for mitochondrial diseases. *J. Mol. Med.*, **98**, 1467–1478.
68. Fujita,Y., Ito,M., Kojima,T., Yatsuga,S., Koga,Y. and Tanaka,M. (2015) GDF15 is a novel biomarker to evaluate efficacy of pyruvate therapy for mitochondrial diseases. *Mitochondrion*, **20**, 34–42.
69. Yatsuga,S., Fujita,Y., Ishii,A., Fukumoto,Y., Arahata,H., Kakuma,T., Kojima,T., Ito,M., Tanaka,M., Saiki,R. *et al.* (2015) Growth differentiation factor 15 as a useful biomarker for mitochondrial disorders. *Ann. Neurol.*, **78**, 814–823.